Spatial and temporal dynamics of organohalide-respiring bacteria in a heterogeneous PCE–DNAPL source zone

Natalie L. Cápiro [a], Frank E. Löffler [b,c,d,e], Kurt D. Pennell [a]

[a] Department of Civil and Environmental Engineering, Tufts University, Medford, MA 02155, United States
[b] Department of Microbiology, University of Tennessee, Knoxville, TN 37996, United States
[c] Department of Civil and Environmental Engineering, University of Tennessee, Knoxville, TN 37996, United States
[d] Center for Environmental Biotechnology, University of Tennessee, Knoxville, TN 37996, United States
[e] University of Tennessee and Oak Ridge National Laboratory (UT-ORNL) Joint Institute for Biological Sciences (JIBS) and Biosciences Division, Oak Ridge National Laboratory, Oak Ridge, TN 37831, United States

Abstract

Effective treatment of sites contaminated with dense non-aqueous phase liquids(DNAPLs) requires detailed understanding of the microbial community responses to changes in source zone strength and architecture. Changes in the spatial and temporal distributions of the organohalide-respiring *Dehalococcoides mccartyi* (Dhc) strains and *Geobacter lovleyi* strain SZ (*Geo*SZ) were examined in a heterogeneous tetrachloroethene-(PCE-) DNAPL source zone within a two-dimensional laboratory-scale aquifer flow cell. As part of a combined remedy approach, flushing with 2.3 pore volumes (PVs) of 4% (w/w) solution of the nonionic, biodegradable surfactant Tween® 80 removed 55% of the initial contaminant mass, and resulted in a PCE–DNAPL distribution that contained 51% discrete ganglia and 49% pools (ganglia-to-pool ratio of 1.06). Subsequent bioaugmentation with the PCE-to-ethene-dechlorinating consortium BDI-SZ resulted in *cis*-1,2-dichloroethene (*cis*-DCE) formation after 1 PV (ca. 7 days), while vinyl chloride (VC) and ethene were detected 10 PVs after bioaugmentation. Maximum ethene yields (ca. 90 μM) within DNAPL pool and ganglia regions coincided with the detection of the *vcrA* reductive dehalogenase (RDase) gene that exceeded the *Dhc* 16S rRNA genes by 2.0 ± 1.3 and 4.0 ± 1.7 fold in the pool and ganglia regions,

respectively. *Dhc* and *Geo*SZ cell abundance increased by up to 4 orders-of-magnitude after 28 PVs of steady-state operation, with 1 to 2 orders-of-magnitude increases observed in close proximity to residual PCE–DNAPL. These observations suggest the involvement of these dechlorinators in the observed PCE dissolution enhancements of up to 2.3 and 6.0-fold within pool and ganglia regions, respectively. Analysis of the solid and aqueous samples at the conclusion of the experiment revealed that the highest VC ($\geq$ 155 μM) and ethene ($\geq$ 65 μM) concentrations were measured in zones where *Dhc* and *Geo*SZ were predominately attached to the solids. These findings demonstrate dynamic responses of organohalide-respiring bacteria in a heterogeneous DNAPL source zone, and emphasize the influence of source zone architecture on bioremediation performance.

1. Introduction

Chlorinated solvent releases continue to pose long-term remediation challenges, particularly at sites where these contaminants exist as dense non-aqueous phase liquids (DNAPLs) (NRC, 2013, Stroo et al., 2012). Despite considerable progress in the development and testing of in-situ remediation technologies over the last 25 years, removing sufficient DNAPL mass to achieve concentration-based cleanup goals remains technically challenging at many sites (Kueper et al., 2014, NRC, 2013, Stroo et al., 2012). The difficulties encountered during DNAPL site remediation can often be related to the heterogeneous distribution of contaminant mass. For example, a DNAPL source zone may contain regions of discrete DNAPL droplets (i.e., ganglia) and higher-saturation "pools" residing above lower permeability lenses or confining layers. While higher specific surface area droplets and ganglia are more amenable to dissolution-based processes, DNAPL pools can persist in the subsurface for decades or centuries, serving as long-term sources of groundwater contamination (NRC, 2013).

Bioaugmentation and biostimulation have emerged as reliable technologies for treating chlorinated solvents sites (Lyon and Vogel, 2013, Pandey et al., 2009) due to an improved understanding of microbial processes, in particular *Dehalococcoides mccartyi* (*Dhc*) strains that detoxify chlorinated ethenes to ethene (Löffler et al., 2013a, Löffler et al., 2013b). Microbial reductive dechlorination provides an effective means for DNAPL source zone treatment, either as a standalone technology (Adamson et al., 2003, Haest et al., 2012, Philips et al., 2012, Sleep et al., 2006) or combined with physical–chemical technologies as a "polishing" step (Christ et al., 2005, Fletcher et al., 2011, Mravik et al., 2003, Ramsburg et al., 2004). Numerous studies have demonstrated that dechlorinating bacteria can be active in close proximity to DNAPL, leading to

enhanced dissolution (1.5- to 14-fold enhancement over abiotic dissolution) (Amos et al., 2008, Amos et al., 2009, Glover et al., 2007, Haest et al., 2012, Philips et al., 2013, Sleep et al., 2006, Yang and McCarty, 2000, Yang and McCarty, 2002). Bioenhanced dissolution has the potential to accelerate depletion of source zone contaminant mass, thereby reducing source zone longevity, remediation time and cost. In addition to the challenges associated with the delivery of sufficient electron donor to the contaminant source zone (Löffler and Edwards, 2006, Yang and McCarty, 2000) and inconsistent supply of reducing equivalents (Chu et al., 2004, Da Silva et al., 2006, Yang and McCarty, 2002), DNAPL source zone architecture (Amos et al., 2008, Christ et al., 2005, Christ et al., 2010, Glover et al., 2007, Park and Parker, 2008, Stroo et al., 2012) may influence microbial reductive dechlorination activity and bioenhanced dissolution.

Aquifer cell studies provide a more realistic representation of subsurface conditions compared to microcosms (Amos et al., 2007, McGuire and Hughes, 2003) and homogeneous one-dimensional flow systems (Amos et al., 2008, Amos et al., 2009, Azizian et al., 2008). For example, Sleep et al. (2006)observed growth of *Dhc* in close proximity to a tetrachloroethene- (PCE-) DNAPL source where aqueous concentrations exceeded 700 μM (115 mg/L), resulting in microbially-enhanced dissolution. Haest et al. (2012) hypothesized that non-uniform mixing of water and pooled trichloroethene (TCE) due to variable DNAPL configuration may have a greater influence on the dissolution enhancement factor than the biodegrading microbes. However, assessment of the DNAPL distribution in that study was based on visual observations (Oil-Red-O was used to dye DNAPL) and measured concentrations of chlorinated ethenes rather than direct measurement of DNAPL saturations. Investigations of the influence of DNAPL saturation on reductive dechlorination and bioenhanced dissolution have been largely based on mathematical models (Parker and Park, 2004), or were conducted in small

test cells with uniform saturation (Glover et al., 2007). Experimental investigations have not considered the effects of changes in DNAPL source zone architecture on spatial and temporal distributions and activity of dechlorinating populations, and the distribution of microbes between the solid and aqueous phases, which has implications on the feasibility of monitored natural attention (MNA) and the success of enhanced bioremediation (Cápiro et al., 2014, Lu et al., 2006, Ritalahti et al., 2010b).

The objective of this study was to improve our understanding of bioremediation within heterogeneous DNAPL source zones as a function of mass removal and source zone architecture. A laboratory-scale aquifer cell was established with a heterogeneous PCE–DNAPL saturation distribution consisting of regions of high saturation pools and discrete ganglia. Following flushing with a nonionic surfactant (4% w/w Tween® 80), which removed 55% of the PCE–DNAPL mass, the aquifer cell was biostimulated with 10 mM lactate and bioaugmented with a PCE-to-ethene dechlorinating consortium as part of a combined remedy approach. Spatial and temporal distributions of the key dechlorinating species *Dhc* and *Geobacter lovleyi* strain SZ (*Geo*SZ) were measured within the aquifer cell. In addition, *Dhc* reductive dehalogenase (RDase) genes and the daughter product formation were monitored within the aquifer cell using sideport samplers. These data were used to determine the extent of bioenhanced dissolution as a function of DNAPL saturation (i.e., ganglia versus pool regions).

2. Materials and Methods

2.1 Aquifer cell setup and preparation

The aquifer cell was constructed with two 1.4 cm thick glass panels held in place by a custom-milled aluminum frame to yield internal dimensions of 63.5 cm (length) × 38 cm

(height) × 1.4 cm (thickness) (Suchomel et al., 2007). Eighteen sampling ports, aligned in four vertical transects of four or five ports, were located within the front glass panel to allow for in-situ quantification of chlorinated ethenes, non-attached (planktonic) biomass, and fermentation products (Fig. 1). The aquifer cell was packed under water-saturated conditions with a 1:1 (w/w) mixture of 20–30 mesh and 40–50 mesh Accusand as the porous medium. Two regions of low permeability lenses consisting of F-70 Ottawa sand were emplaced within the background medium to promote the formation of both pool and ganglia regions. In addition, a 3-cm thick layer of F-70 Ottawa sand was placed at the bottom of the cell to create a lower confining layer (Fig. S-1). Following packing, approximately 40 mL of PCE–DNAPL dyed with Oil-Red-O (0.4 mM) was injected into the aquifer cell (Fig. 1, above port 2A) at a flow rate of 0.5 mL/min using a Harvard Apparatus model 22 syringe pump (Holliston, MA) and allowed to distribute for 24 h. Degassed water containing 3.4 mM $CaCl_2$ (500 mg/L) as the background electrolyte was then flushed through the aquifer cell at a flow rate of 1 mL/min during the initial 5-pore volume (PV, 1 aqueous PV = 1180 mL) plume development period.

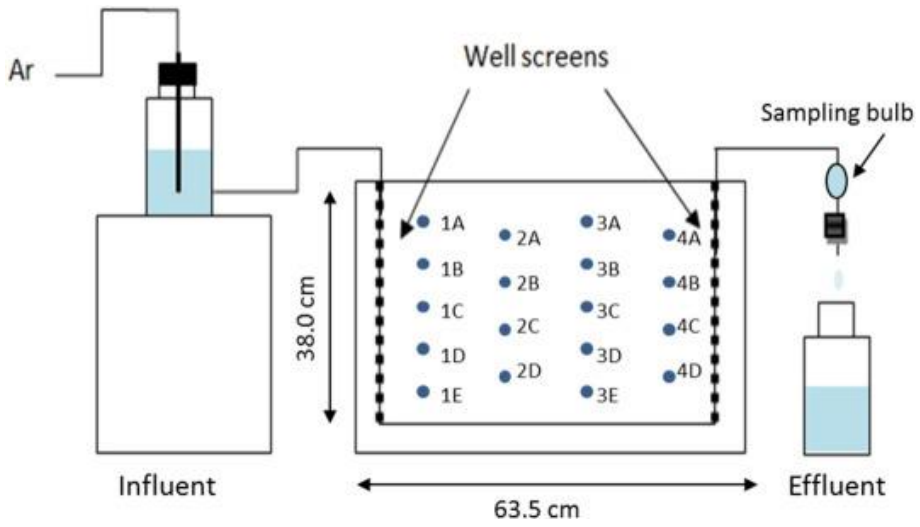

Fig. 1. Aquifer cell configuration with argon-flushed influent, screened inlet and outlet wells, 18 sampling ports, sampling bulb and effluent drip.

The glass panel construction allowed for the quantification of PCE–DNAPL saturation distributions using a light transmission (LT) system (Tidwell and Glass, 1994) described in the Supplemental material. Briefly, thickness-averaged saturations were expressed as pool fraction (PF, 0 to 1) and ganglia-to-pool (GTP, 0 to infinity) ratio (Suchomel and Pennell, 2006), where PCE–DNAPL saturations (S_{PCE}) of less than 13% were considered to represent discrete ganglia within the background matrix, and saturations that were equal to or greater than the residual saturation represented "pools" (see Supplementary material).

2.2. Medium preparation and bioaugmentation

Prior to bioaugmentation, 1 PV of reduced mineral salts medium prepared according to the recipe outlined by Löffler et al. (1996) and Sung et al. (2003)with the modifications incorporated by Amos et al. (2009), and amended with 10 mM lactate as the electron donor was flushed through the aquifer cell to establish anoxic conditions. Bio-Dechlor INOCULUM (BDI-SZ), a non-methanogenic, PCE-to-ethene dechlorinating consortium that contains fermenters,

homoacetogens, and multiple dechlorinators, including three *Dhc* strains and *Geo*SZ (Amos et al., 2009), was used for bioaugmentation. The three *Dhc* strains FL2, GT, and BAV1 harbor the *tceA*, *vcrA*, and *bvcA* reductive dehalogenase (RDase) genes, respectively, and represent 46%, 54%, and < 0.001% of the *Dhc* population in BDI-SZ, respectively. The consortium was maintained for several months with periodic additions of 0.33 mM PCE as electron acceptor and 10 mM lactate as electron donor, and was sampled prior to inoculation for quantitative real-time polymerase chain reaction (qPCR) analysis (see Supplementary material) that yielded initial abundances of $9.81 \pm 0.23 \times 10^7$ *Dhc* cells/mL and $3.66 \pm 1.24 \times 10^7$ *Geo*SZ cells/mL. Cell numbers are reported per milliliter of aqueous phase or scaled to 4.93 g of dry sand (i.e., the amount of dry Accusand background porous medium with a pore volume of 1 mL) to allow for direct comparison of planktonic (i.e., non-attached) and attached cell numbers. Cells associated with the aqueous phase, collected from co-located sideports immediately prior to destructive sampling of the aquifer cell, were subtracted from the total cell numbers measured in wet sand material within the area of withdrawal influence for each sideport to determine solid phase attached cells (Cápiro et al., 2014).

2.3. Aquifer cell influent delivery system

An unconfined flow system with a hydraulic head difference ranging from 0.3 to 3 cm over the length of the aquifer cell (hydraulic gradient of 0.005 to 0.05) was established using a constant head apparatus. Operational flow rates ranged from 0.05 to 1.0 mL/min, corresponding to pore-water (seepage) velocities of 3.9 to 78.5 cm/day and residence times of 0.8 to 17 days. Influent solutions were transferred to a 4 L Mariotte bottle equipped with an aspirator (Ace Glass, Vineland, NJ) connected to a slotted 0.3175 cm O.D. (1/8 in.) stainless steel tubing located inside the fully screened influent end chamber of the aquifer cell. Insertion of 0.635 cm

O.D. (1/4 in.) stainless steel tube into the Mariotte bottle provided for a constant head independent of the volume of water in the reservoir. The aqueous flow rate was controlled by adjusting the heights of the Mariotte bottle and the effluent tubing outlet. Prior to bioaugmentation, the influent delivery system was modified to maintain anoxic conditions by attaching a glass column filled with powdered ferrous iron as in-line oxygen scrubber/absorber (Restek Corporation; Bellefonte, PA) and the headspace was continuously flushed with argon gas. Performance of the oxygen removal system was monitored by addition of the redox indicator resazurin (1 nM, Sigma Aldrich) to the mineral salts medium.

2.4. Aquifer cell operation and sample collection

As part of a combined remedy strategy designed to promote more efficient remediation of the PCE–DNAPL source zone and to create conditions more conducive to bioremediation (e.g., decreased PCE concentrations), a sequence of two 4% (w/w) Tween® 80 surfactant floods (1 + 1.3 PVs, 2.3 total PVs) was conducted at a flow rate of 4 mL/min (3 m/day) to incrementally remove PCE mass via micellar solubilization (Pennell et al., 2014). After each surfactant flood, 20 to 30 PVs of background electrolyte solution (500 mg/L $CaCl_2$) were introduced at 1.0 mL/min. Once flux-averaged PCE effluent concentrations stabilized (63 ± 16.5 mg/L), three PVs of mineral salts medium without electron donor were flushed through the aquifer cell at a flow rate of 0.15 mL/min (ca. 6-day residence time) to establish anoxic conditions prior to bioaugmentation. Following the injection of one PV of medium amended with 10 mM lactate, 20 mL of the BDI-SZ consortium was introduced into each of the nine sideports located upgradient from and within the source zone using a gas-tight syringe (first two transects, ports 1A–1E and 2A–2D, Fig. 1). For the remainder of the experiment, medium with 10 mM lactate

was flushed through the aquifer with a 6 to 10 day residence time (i.e., 0.15 to 0.1 mL/min). A timeline of aquifer cell operation is presented in Table 1.

Flux-averaged effluent samples were collected every 0.1 to 0.3 PVs, and sideport samples were collected every 1 to 4 PVs. The effluent collection system consisted of a 20-mL glass sampling bulb that allowed for the analysis of chlorinated ethenes, ethene and pH, and following bioaugmentation, organic acids and bacterial cells. Biomass was collected from aqueous samples (1–1.5 mL) withdrawn from each sampling port and the effluent (15 mL). Following collection of the final round of aqueous samples from the sideports at the termination of the experiment (day 525, PV 116.2; Table 1), solid phase samples were obtained from a 1 cm radius around each sideport by destructive sampling. To enumerate dechlorinating bacteria by qPCR, DNA was extracted from solid and aqueous samples following established protocols (described in the Supplemental material) (Amos et al., 2009, Cápiro et al., 2008, Cápiro et al., 2014).

3. Results and Discussion

3.1. DNAPL source characterization and plume development

After PCE–DNAPL release into the aquifer cell and the initial plume development period (5 PV electrolyte solution flush, Fig. S-2), the resulting GTP ratio and the PF in the source zone were 1.6 and 0.38, respectively. These data indicate that approximately 62% of the PCE–DNAPL volume consisted of entrapped ganglia, while the remaining 38% corresponded to higher-saturation pools ($S_{PCE} \geq 0.13$). Following two surfactant floods (2.3 PVs of 4% Tween® 80), approximately 28% and 17% of the initial PCE mass was removed, and flux-averaged effluent concentrations of PCE decreased from 1200 μM to 780 μM and then to 480 μM following the first and second surfactant floods, respectively (Fig. S-2). After each

surfactant flood, the PCE–DNAPL saturation distribution was quantified using the LT system, which indicated that the GTP ratio decreased incrementally from 1.60 to 1.38 (first surfactant flood) and from 1.37 to 1.07 (second surfactant flood). After an additional 25 PVs of $CaCl_2$electrolyte solution (PV 58), (Fig. S-1), the GTP ratio and the PF in the source zone were 1.04 and 0.49, respectively, indicating that approximately half of the PCE–DNAPL volume consisted of entrapped ganglia, while the remaining 50% corresponded to higher-saturation pools. The local dissolved phase PCE concentrations emanating from these DNAPL zones immediately prior to bioaugmentation (PV 73) are shown in Fig. 2. Flux-averaged effluent Tween® 80 concentrations decreased to less than 200 mg/L prior to medium introduction (PV 58) and approached 50 mg/L by PV 64.1 (day 58, Table 1), which is below the level of 250 mg/L Tween® 80 observed to have adverse impact on reductive dechlorination of PCE to ethene by the BDI-SZ consortium (Amos et al., 2007).

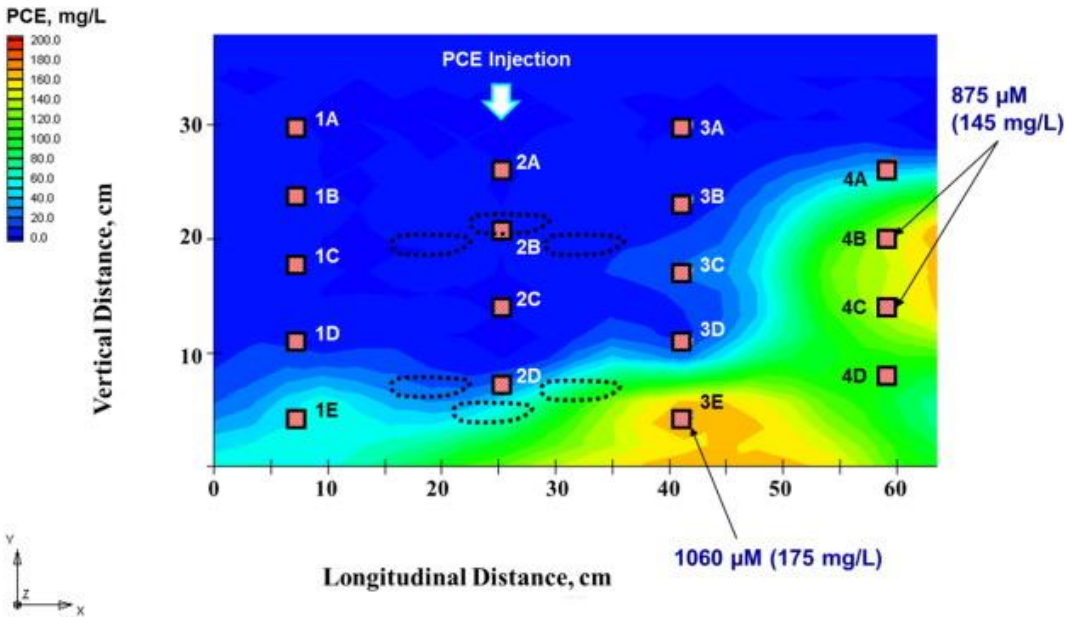

Fig. 2. Contoured spatial distribution of aqueous PCE concentrations measured from sideports (red squares) resulting from dissolution of pools and ganglia following surfactant flushing and prior to bioaugmentation (PV

73). Locations of low permeability lens (F-70 Ottawa sand) are outlined with dotted lines near ports 2B and 2D. Contours calculated using constant natural-neighbors methods with Groundwater Modeling System (GMS).

Within 4 PVs of introducing the mineral salts medium and bioaugmentation with the BDI-SZ consortium (prior to the detection of ethene), a visible black precipitate formed throughout the aquifer cell. Therefore, subsequent monitoring of the PCE source zone mass removal was based on aqueous phase effluent samples rather than LT analysis. The black precipitate was attributed to the formation of iron(II) sulfide (FeS) due to bacterial reduction of ferric iron associated with the porous medium and the introduction of sulfur compounds(e.g., sodium sulfide) in the medium. Eleven PVs post bioaugmentation, the flow rate in the aquifer cell decreased from 185 mL/day to 75 mL/day, which corresponded to an overall relative permeability reduction of 65 ± 11%, attributed to precipitate formation and biomass growth. Acetylene, a product of abiotic PCE reductive dechlorination mediated by FeS (Butler and Hayes, 2001), was monitored according to previously described procedures (Costanza et al., 2009), but not detected throughout the experiment. Therefore, observed PCE degradation was attributed to microbial activity.

3.2. DNAPL dissolution following bioaugmentation

Within 12 PVs after bioaugmentation, flux-averaged effluent PCE concentrations decreased from ca. 300 μM to below 3 μM, TCE (detected after 0.5 PV) concentrations averaged 14.9 ± 23 μM before decreasing below 3.8 μM, and *cis*-DCE (detected after 1 PV) increased to a maximum concentration of 292 μM (Fig. 3). However, VC and ethene were not consistently detected until 10 PVs after bioaugmentation, likely due to an adaption time required by *Dhc* harboring the vinyl chloride reductase (*vcrA*) gene (Damgaard et al., 2013b), and/or

inhibition by PCE and *cis*-DCE (Amos et al., 2009, Damgaard et al., 2013a). The pH of the phosphate-buffered (10 mM) influent medium was 7.2 ± 0.25 throughout the experiment (data not shown); however, the effluent pH dropped to 6.8 (6.5 PVs after bioaugmentation) during periods of lactate (and residual surfactant) fermentation and extensive PCE to *cis*-DCE transformation. This small pH decrease may have delayed vinyl chloride (VC) and ethene production since the optimal pH range for *Dhc* activity is 7.2–7.4 (He et al., 2003). Once the pH approached 7.2 10 PVs after bioaugmentation, VC and ethene were detected consistently, and concentrations increased to 43.5 μM and 31.3 μM, respectively (Fig. 3). Under steady-state conditions (8.0 ± 3.5 cm/day seepage velocity) and 29 PVs after bioaugmentation, the effluent was composed of *cis*-DCE (52.9 μM), VC (25.1 μM) and ethene (17.9 μM), corresponding to an effluent molar composition of 55%, 26% and 19%, respectively (Fig. 3).

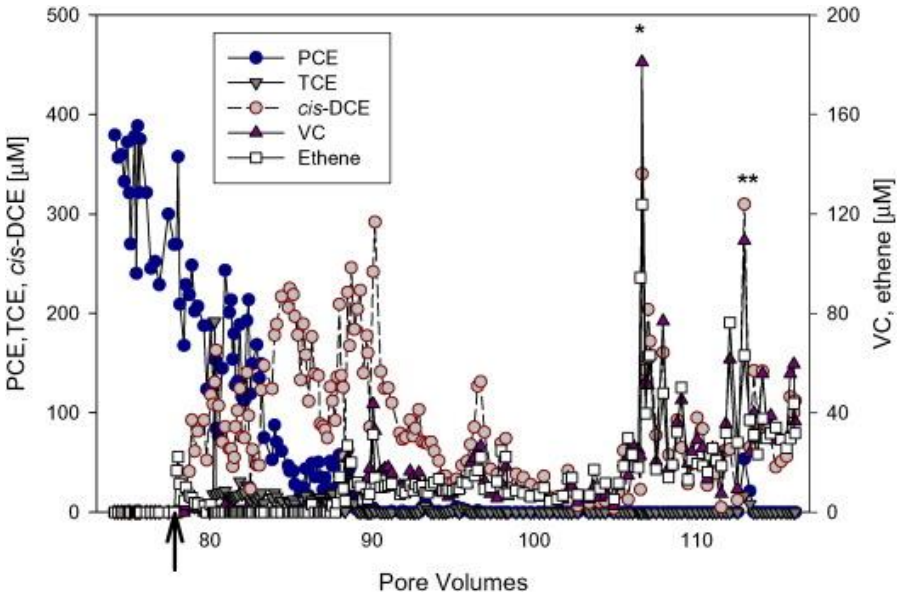

Fig. 3. Flux-averaged effluent chlorinated ethenes and ethene concentrations following reduced medium addition (74.2 PV) and bioaugmentation (77.5 PV, indicated by the arrow). The stars indicate flow interruptions, the first of 14-days after 106.5 PVs (*) and the second of 21-days after 112.5 PVs (**).

A 14-day flow interruption was initiated 29 PVs after bioaugmentation (106.4 PVs overall) to evaluate the potential impacts of mass transfer limitations and hydraulic retention time on dechlorination performance. Upon resuming flow, effluent concentrations of *cis*-DCE (340 μM), VC (181 μM) and ethene (124 μM) exceeded levels measured prior to the flow interruption by up to 7-fold (Fig. 3). After introducing an additional 5 PVs of reduced mineral salts medium (34 PVs following bioaugmentation, 111 PVs overall), effluent concentrations of *cis*-DCE, VC and ethene decreased to 38.3 μM, 25.8 μM and 25.6 μM, respectively. A second 21-day flow interruption, initiated 35 PVs after bioaugmentation (PV 112.5), resulted in an effluent molar composition of *cis*-DCE, VC and ethene shift to 24%, 19% and 57%, respectively. Elevated effluent concentrations of *cis*-DCE (310 μM), VC (109.3 μM), ethene (76 μM), as well as PCE (53.2 μM) and TCE (16.7 μM) were measured after flow resumed, which corresponded to a 7.8-fold enhancement in molar mass removal over pre-flow-interruption measurements.

The marked improvement in dechlorination activity immediately following periods of flow interruption and sustained improvements during subsequent operation indicate that the residence time in the aquifer cell was not sufficient to achieve complete reductive dechlorination to ethene. Unlike the flow interruption initiated during the abiotic phase of the experiment (PV 18.2, 13-days, Table 1) when no mass transfer enhancement was measured, the added residence time promoted more complete transformation of PCE to lesser-chlorinated, more soluble daughter products. This finding is consistent with results from previous continuous-flow column (Amos et al., 2009, Haest et al., 2011) and pilot-scale aquifer tank (Da Silva et al., 2006) experiments that attributed insufficient residence time as a contributing factor for incomplete PCE/TCE reductive dechlorination.

In addition to residence time, the heterogeneous DNAPL saturation distribution in the aquifer cell may have influenced the measured aqueous dissolution beyond the mass transfer limitations associated with specific interfacial (surface) area. Specifically, PCE daughter products (e.g., *cis*-DCE) could have partitioned into PCE–DNAPL located in downgradient regions of the aquifer cell. This partitioning could have led to lower detection of daughter products in the aqueous phase, and thus, underestimates of dechlorination and bioenhancement. Previous studies have demonstrated that partitioning of PCE daughter products is reversible and is not strongly rate limited (Ramsburg et al., 2010, Ramsburg et al., 2011). Based on the NAPL mass that remained in the aquifer cell at the conclusion of the experiment, a NAPL saturation of approximately 0.025 was estimated for the bottom 5–6 cm of aquifer cell. Using daughter product partition coefficients (K_p) of 348 and 593 for VC and *cis*-DCE, respectively (Ramsburg et al., 2010), the retardation factor would be approximately 8 to15, respectively, through the region of the aquifer cell where NAPL existed near the end of experiment. Although partitioning of daughter products into entrapped NAPL was not thought to be important in this system, the process should be considered when evaluating bioremediation in heterogeneous source zones containing DNAPL.

The remaining chlorinated ethene mass was measured by destructively sampling the aquifer cell immediately after flow was stopped (116.2 PV). Approximately 14% of the originally emplaced PCE mass was recovered in methanol extracts of the aquifer cell solids. Combined with 55% PCE mass removal achieved during the surfactant flushing and the 15% equivalent mass (molar summation of all chlorinated ethenes and ethene) eluted during the biological transformation phase, the total experimental mass balance was 84%. The remaining 16% of PCE mass that was not accounted for could be attributed to a number of factors including

(i) volatile losses of parent and daughter products, especially VC and ethene through the upper surface of the aquifer cell which did not have a gas-tight seal (ii) accumulation of small amounts of PCE–NAPL in three of the sampling ports, which was observed visually, and (iii) unintentional removal of PCE–DNAPL during side port sampling events. Nevertheless, the aquifer cell system allowed for detailed monitoring of contaminant concentrations and distributions of the key dechlorinators for over 1 year.

3.3. Temporal and spatial distribution of *Dhc* and *Geo*SZ

Dhc cell numbers measured in aqueous sideport samples collected 28.9 PVs after bioaugmentation increased by 1 to 4 orders-of-magnitude compared to titers measured after 4.5 PVs within the ganglia regions of the source zone (Fig. 4A). Across the four-port transects, cell titers increased with proximity to the PCE-DNAPL, and were 1 to 2 orders-of-magnitude higher than those measured in the upper half of the aquifer cell (Fig. 4A), which contained minimal PCE–DNAPL (Fig. 2). Following the first flow interruption period (PV 106.4), *Dhc* cell numbers increased up to 2.8×10^8 cells/mL, and up to 3 orders-of-magnitude above titers measured during operational flow conditions (PV 82) at port 3E near the remaining DNAPL pool (Fig. 4A). After 116 PVs of operation, *Dhc* cell numbers decreased below the levels measured immediately following the flow interruption periods at most sample locations, yet the cell numbers exceeded those measured pre-interruption, indicating that the temporary flow stoppage stimulated *Dhc* growth. During bioremediation field applications, hydraulic control to achieve periods of reduced flow within the source zone could help to increase *Dhc* cell numbers, and in turn, enhance dechlorination performance within the source zone.

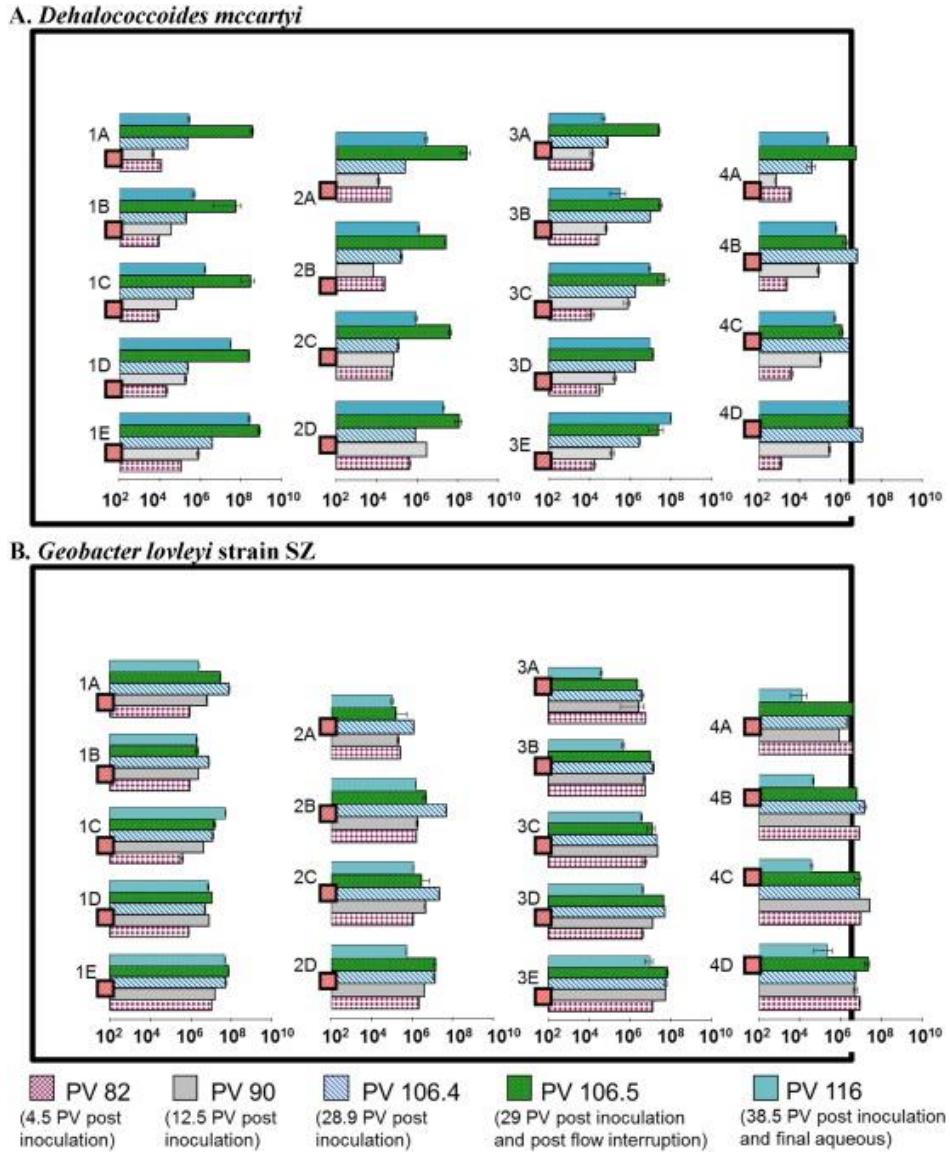

Fig. 4. Spatial distribution of total planktonic *Dhc* (A.) and *Geo*SZ (B.) (cells per mL) measured after inoculation (PV 82), after the detection of VC and ethene (PV 90), immediately before the first flow interruption (PV 106.4), after the first flow interruption (PV 106.5), and at the conclusion of the experiment (PV 116).

*Geo*SZ planktonic cell numbers increased 1 to 2 orders-of-magnitude (up to 1.6×10^8 cells/mL) during steady flow, with the highest cell numbers observed in close proximity to the zones of high-saturation PCE–DNAPL (Figs. 4B and S-1). The detection of increased *Geo*SZ cell numbers in the source zone is consistent with the conversion of PCE to *cis*-

DCE in the lower third of the aquifer cell (D and E ports, Fig. 1), and coincides with observations made in a column experiment with the same inoculum, where 3.5-fold higher *Geo*SZ cell numbers were measured near the source zone compared to the downgradient plume region (Amos et al., 2009). The additional contact time provided by the flow interruptions at PV 106.4 increased *Geo*SZ cell titers by no more than 1 order-of-magnitude near the source zone, and at most locations, cell titers declined by up to 1 order-of-magnitude. The decrease in *Geo*SZ titers corresponded to low levels (or absence) of electron acceptors (PCE and TCE), which were only detected at sampling ports 1E and 3E (Fig. 1, Fig. 2) at the conclusion of the experiment. Sideport measurements confirmed that *Geo*SZ was not electron donor limited as acetate (used by *Geo*SZ to transform PCE to *cis*-DCE, Sung et al., 2006a) levels exceeded 2 mM in all sample locations.

3.4. Dechlorinator activity and growth within the pool and ganglia regions

A detailed analysis of the dechlorinating populations was performed at two sideport locations, 3E and 4D (Fig. 1, Fig. 2). Sampling port 3E, which consistently showed the highest PCE and *cis*-DCE concentrations, was selected to assess microbial activity in the vicinity of pooled PCE–DNAPL ($S_{PCE} \geq 13\%$). Sampling port 4D, which was located in a region of entrapped ganglia, was selected due to high PCE concentrations and evidence of consistent reductive dechlorination to VC and ethene.

Dechlorination in DNAPL pool regions near port 3E was apparent based on the change in composition of aqueous phase chlorinated ethenes and ethene concentrations, which transitioned over time from primarily PCE (1076 μM) to predominately *cis*-DCE (up to 1512 μM) with some VC and ethene (Fig. 5A). *Geo*SZ cell titers coincided with PCE depletion and *cis*-DCE formation. *Dhc* cell numbers followed a similar trend to *Geo*SZ over time, but were consistently

2 orders-of-magnitude lower, representing 2% or less of the dechlorinating community (i.e., the sum of *Dhc* strains and *Geo*SZ cells) prior to the first flow interruption (PV 106.4, Table 1 and Table S-1 in Supplemental material). Following the first flow interruption, *Dhc* and *Geo*SZ cell numbers increased, and the fraction of *Dhc* cells increased to 15% (Table S-1). Similar increases in *Dhc* cells (from 7 to 12%) were detected after the second flow interruption at PVs 112.5 (Table S-1). At the conclusion of the experiment, *Dhc* cell numbers had increased by nearly 2 orders-of-magnitude from before initiation of the flow-interruptions and represented 84% of the total dechlorinators detected at port 3E, while *Geo*SZ maintained a relative constant titer of $1.6 \pm 0.5 \times 10^7$ cells/mL (Table S-1). Unlike other studies that have shown limited VC and ethene production in regions of high PCE and/or *cis*-DCE concentrations (up to 1 mM) (Adamson et al., 2003, Glover et al., 2007, Sleep et al., 2006), the observed increases of *Dhc* cells within this PCE–DNAPL pool region are consistent with the observed formation of VC and ethene, which reached concentrations of 132 μM and 85 μM, respectively.

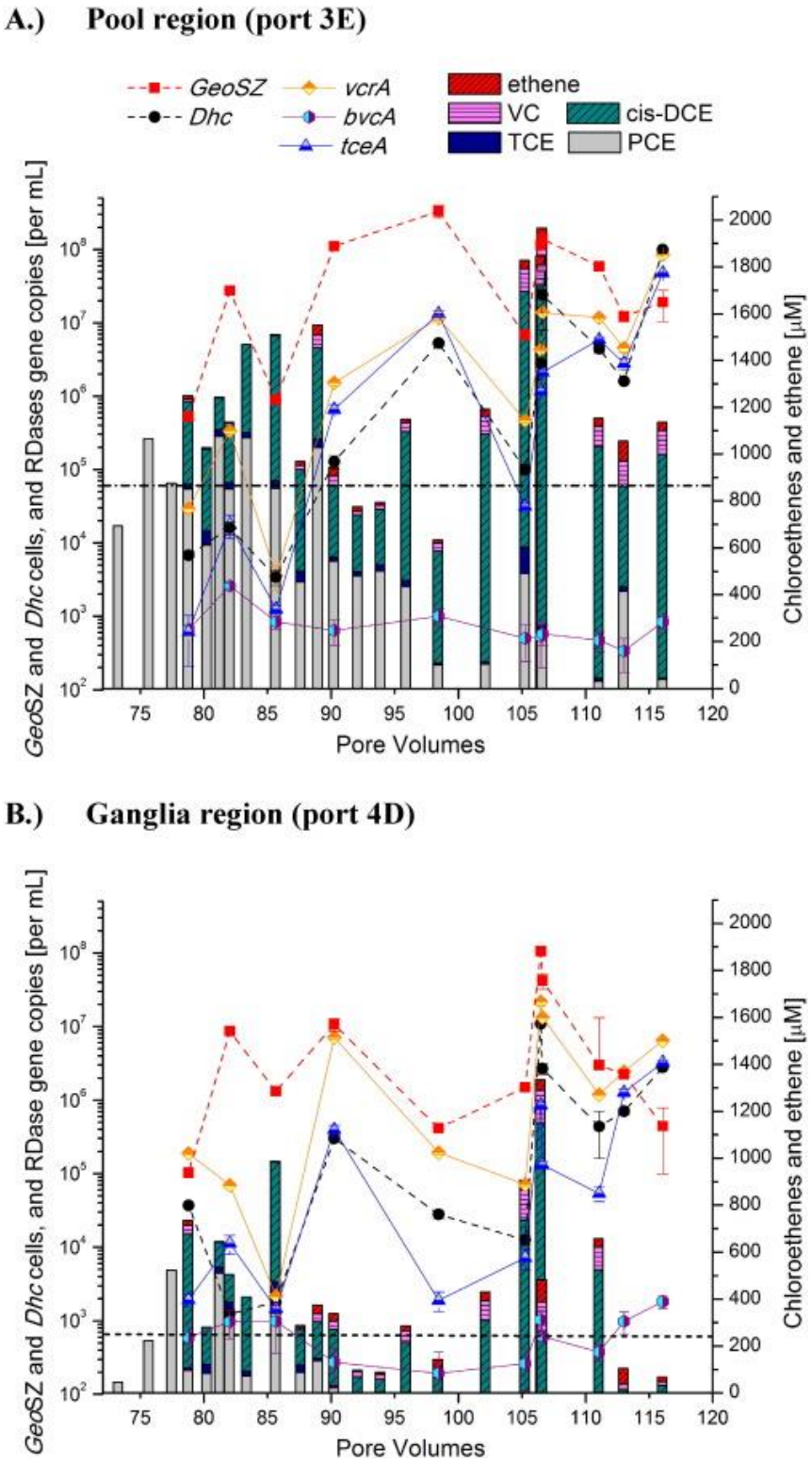

Fig. 5. Dechlorinators (*Dhc* and *Geo*SZ), *Dhc* RDase genes and dissolved chlorinated ethenes and ethene measured from the source zone: A.) pool region (port 3E) and B.) ganglia region (port 4D). Horizontal dashed

lines represent the average molar concentration of PCE measured over the 10 PVs prior to bioaugmentation that was used to distinguish bioenhanced vs. abiotic dissolution.

In the ganglia region (port 4D), growth of dechlorinators correlated with measured concentrations of chlorinated ethenes and ethene, yet the cell numbers were generally one order-of-magnitude lower than those measured near the pool region (Fig. 5B and Table S-1). The effects of the flow interruption at PV 106.4 in the ganglia region (port 4D) were not as pronounced compared to the pool location (port 3E) (Table S-1). However, reductive dechlorination following the first flow interruption increased VC and ethene amounts from 11% and 3% (mole/mole) to over 26% and 19% of the total aqueous phase chlorinated ethenes and ethene, respectively. Similarly, before the second interruption at PV 112.5, the aqueous molar concentrations of VC and ethene were 15% and 6% (mole/mole), and increased to 21% and 65%, respectively. With the depletion of PCE and TCE (electron acceptors for *Geo*SZ) within ganglia and upgradient DNAPL pool regions, *Dhc* cell numbers increased one order-of-magnitude at the conclusion of the experiment (PV 116), representing 86% of the total dechlorinators present at port 4D. Consistent with the depletion of PCE and TCE, *Geo*SZ decreased by an order-of-magnitude at the conclusion of the experiment compared to the previous measurement at PV 113 (Fig. 5B and Table S-1).

Of the total RDase gene abundance measured near the pool and ganglia regions, the *vcrA* gene implicated in *cis*-DCE and VC dechlorination to ethene (Müller et al., 2004, Sung et al., 2006b) was consistently the most prevalent with 76 ± 16% and 87% ± 16%, respectively, of the total RDase genes (Fig. 5, Table S-2). The *tceA* gene, implicated in TCE to VC reductive dechlorination (Magnuson et al., 2000) represented 23 ± 16% and the *bvcA* gene (DCEs and VC to ethene) (Krajmalnik-Brown et al., 2004) represented 2 ± 4% of the total RDase genes in the

pool region. In the ganglia region, the *tceA* gene abundance was lower than in the pool region, representing 10% ± 12% of the total RDase genes measured, presumably due to the decreased availability of TCE and *cis*-DCE within this zone. The *bvcA* gene titers also remained low in the ganglia region, representing less than 2% ± 6% of the total RDase gene abundance. Interestingly, the *vcrA* gene copy numbers generally exceeded the *Dhc* 16S rRNA genes by 2.0 ± 1.3 and 4.0 ± 1.7 fold in the pool and ganglia regions, respectively, following the production of ethene. An incongruity between *Dhc* 16S rRNA gene and RDase gene numbers has been observed previously (Damgaard et al., 2013a, van der Zaan et al., 2010), but the relative overabundance of *vcrA* genes is difficult to rationalize based on the current understanding of *Dhc* biology (i.e., occur as single copy genes on the known *Dhc* genomes).

3.5. Bioenhanced DNAPL dissolution

The maximum bioenhancement factor for the representative pool and ganglia regions (ports 3E and 4D, discussed above) was determined by comparing the total measured molar concentrations of chlorinated ethenes and ethene to the average molar concentration of PCE measured during the 10 PVs prior to bioaugmentation (i.e., dissolution under abiotic conditions). PCE concentrations of 849 ± 163 μM and 223 ± 214 μM for the pool (port 3E) and ganglia (port 4D), respectively, rather than the PCE solubility (i.e., 1200 μM) were used for this comparison because the source zone architecture did not allow for ideal dissolution to occur, and thus, effluent samples were diluted. After the first flow interruption, 2.3-fold and 6-fold enhancements over abiotic dissolution were measured within the pool (port 3E) and ganglia (port 4D) regions, respectively. Following the second flow interruption, DNAPL dissolution was enhanced 1.4-fold and 3.0-fold, respectively (Fig. 5). The reduction in bioenhanced dissolution between the first and the second flow interruption periods coincided with a decrease in local PCE and TCE

concentrations. Based on the total molar mass of chlorinated ethenes and ethene recovered, the cumulative enhancement in PCE dissolution over the duration of the biologically active phase of the experiment was 1.11-fold and 1.68-fold near the high-saturation pool (port 3E) and ganglia regions (port 4D), respectively. These bioenhancement calculations are considered conservative because the values were referenced against steady-state abiotic conditions determined at early time when high-surface area ganglia were more prevalent in the aquifer cell.

These maximum and cumulative bioenhancement factors are on the lower end of previously reported values, which range from 1.5 to 21-fold and 1.3 to 6.5-fold, respectively (Adamson et al., 2003, Amos et al., 2008, Amos et al., 2009, Glover et al., 2007, Harkness and Fisher, 2013, Philips et al., 2012, Philips et al., 2013, Sleep et al., 2006, Yang and McCarty, 2000, Yang and McCarty, 2002). Numerous factors influence calculated values of bioenhanced dissolution, including pore-water velocity, electron donor supply, degradation kinetics, distribution and configuration (i.e., architecture) of the DNAPL source zone, and contaminant concentrations and availability (Amos et al., 2009, Christ and Abriola, 2007, Chu et al., 2003, Chu et al., 2004, Glover et al., 2007). Many prior studies used a source zone composed only of residual NAPL (Yang and McCarty, 2000, Yang and McCarty, 2002) and/or utilized a mixed-NAPL that consisted of the target constituent (TCE or PCE) dissolved in an innocuous NAPL phase (i.e., hexadecane) in order to decrease or limit the maximum aqueous phase PCE or TCE concentrations emanating from the source (Amos et al., 2008, Amos et al., 2009, Cope and Hughes, 2001, Zheng et al., 2001). However, when compared to aquifer cell studies utilizing a neat PCE- (Sleep et al., 2006) or TCE- (Haest et al., 2012) DNAPL source zone, the observed enhancement factors were similar (1.01–1.7 cumulative, 1.3–3.3 maximum), suggesting that lower enhancement factors should be anticipated in more realistic, heterogeneous source zones.

3.6. Final distribution of *Dhc* and *Geo*SZ cells between aqueous and solid phases

At the conclusion of the aquifer cell experiment (116.2 PVs), the enumeration of *Dhc* and *Geo*SZ cells in aqueous sideport and solid (sand) phase samples revealed heterogeneous distributions of these dechlorinators (Fig. 6). Throughout the aquifer cell, non-attached *Dhc* and *Geo*SZ cells accounted for an average of 24% ± 14% and 14% ± 12% of the total cell numbers (i.e., non-attached plus attached), respectively. Both the absolute cells numbers associated with both phases (co-located aqueous and solid phase samples) and the fraction of cells associated with the solid phase generally increased with proximity to residual PCE–DNAPL. In locations that contained DNAPL pool regions (ports 1E and 3E, Fig. 6), *Geo*SZ cells were measured predominately attached (11–17% non-attached). In these same locations, the highest concentrations of VC (156 μM) and ethene (66 μM) were measured, indicating that *Dhc* was active; *Dhc* cells in these remaining pool regions were primarily attached (28–39% non-attached). In downgradient zones with residual PCE ganglia (ports 2D and 4D), *cis*-DCE (≤ 120 μM), VC (≤ 40 μM) and ethene (≤ 30 μM) were detected, and *Dhc* and *Geo*SZ were also predominately attached (6–11% and 3%, respectively, non-attached).

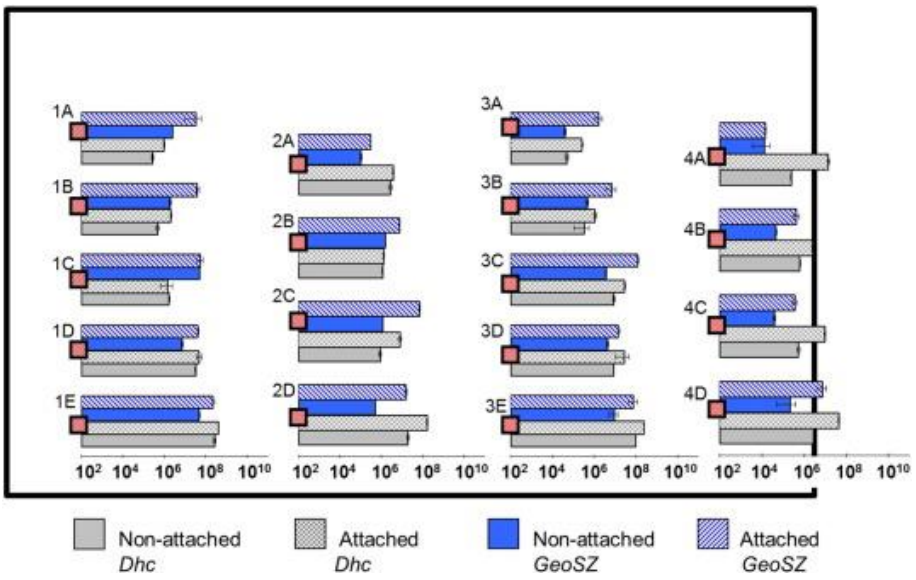

Fig. 6. Final spatial distribution of *Dhc* and *Geo*SZ of non-attached (cells per mL) and attached (cells per 4.93 g sand [the amount of sand with 1 mL pore volume]) cells.

Numerous studies have shown that microbial cell distribution between the aqueous and solid phases is a species-specific, dynamic process influenced by several factors including geochemical conditions (e.g., ionic strength, pH), contaminant concentrations, nutrient availability, physiological state of the organisms, hydrodynamic shear forces, and properties of the solid matrix (e.g., permeability, surface charge) (Alfreider et al., 1997, Amos et al., 2009, Fontes et al., 1991, Holm et al., 1992, Lehman, 2007, Lehman et al., 2001, Liu and Tay, 2002, Pedersen and Ekendahl, 1990, Reardon et al., 2004, Schaefer et al., 2010, Scholl et al., 1990, Thomas et al., 2002, Zhang and Olson, 2012). These environmental conditions and organismal properties may lead to bacterial cell attachment distributions ranging from predominately associated with the aquifer solids to predominately associated with the aqueous phase (i.e., planktonic) (Balkwill and Ghiorse, 1985, Bekins et al., 1999, Fennell et al., 2001, Godsy et al., 1992, Haest et al., 2011, Hazen et al., 1991, Lehman et al., 2001, Reardon et al., 2004, Schaefer et al., 2009). The aquifer cell results demonstrated that in near source zone

regions (i.e., electron acceptor available) with sufficient electron donor supply, bioaugmented *Geo*SZ and *Dhc* were preferentially associated with the solid phase after more than 1 year of biostimulation. Previous work with the same culture over a shorter timeframe also demonstrated preferential distribution of *Dhc* and *Geo*SZ when electron acceptor and donor were available; however, the culture was primarily planktonic when electron donor was limiting (Cápiro et al., 2014). Further, the results presented here indicate that the fraction of attached and non-attached cells varies with distance from the DNAPL source, and to a lesser extent DNAPL saturation (e.g., high saturation pools vs. regions of lower saturation ganglia). Proximity to the source zone has been shown to affect the distribution between attached versus non-attached cells (Amos et al., 2009), and may account for differences in the fraction of attached cells detected in laboratory studies compared to field sampling that typically occur at greater distances from the actual DNAPL source. Overall, the measurements of cell phase distribution in the aquifer cell provide additional evidence that reliance on groundwater samples alone could render estimates of dechlorination activity (e.g., time required for cleanup) unreliable if *Dhc* are under the 10^6 cells/L threshold for probable ethene formation (Löffler et al., 2013a, Lu et al., 2006, Ritalahti et al., 2010a). Thus, cell abundance measurements in the aqueous phase should be interpreted with caution when predicting enhanced bioremediation or natural attenuation activity.

3.7. Implications for bioremediation

Assessments of site bioremediation potential have rarely considered the impact of source zone architecture and DNAPL saturation on dechlorinating microbial communities. The results of this study demonstrated that heterogeneous DNAPL distributions affect growth and distribution of dechlorinating populations and consequently, biologically enhanced DNAPL

dissolution. In regions consisting predominately of discrete ganglia, up to 100% higher rates of biologically enhanced dissolution were observed compared to areas characterized by high saturation pools. Therefore, when assessing the potential for reductive dechlorination, DNAPL saturation distribution can impact degradation rates, especially under slow groundwater flow conditions (Chu et al., 2004). Further, although both dechlorinating species were predominately attached to the sandy solid phase independent of the DNAPL saturation within the aquifer cell, the results suggest that the abundance of attached cells in regions containing ganglia could exceed pool-dominated regions 4–5 fold, making estimates of the total microbial population (non-attached plus attached) challenging when biomass sample collection relies solely on groundwater. Variability of aqueous phase cells abundances in response to DNAPL saturation could potentially impact the interpretation of qPCR data (Lu et al., 2006, Ritalahti et al., 2010a), in particular when the porous medium has higher organic content (Cápiro et al., 2014).

The outcomes of this study not only emphasize the value of quantitative assessment of *Dhc* cell numbers (i.e., 16S rRNA genes), but also indicate that individual RDase genes may correlate more closely to successful bioremediation (e.g., transformation to ethene). For example, *Dhc* distributions were strain-specific relative to the DNAPL source zones, which a 16S rRNA gene-targeted approach would not resolve. Implementation of bioaugmentation following partial mass removal using an aggressive physical–chemical remedy (e.g., surfactant flushing) was successfully demonstrated. This finding provides further support for combined remedy approaches (i.e., short-term mass removal followed by bioremediation), which could be beneficial at complicated DNAPL sites exhibiting asymptotic steady-state (stalled) mass removal.

4. Conclusions

Monitoring spatial and temporal phase distribution of two key dechlorinating microbial species provided direct evidence of changes and variability in dechlorination activity within a heterogeneous PCE–DNAPL source zone following partial mass removal by Tween® 80 surfactant. This information, along with detailed source zone mass distributions, is essential for the estimation of mass transfer and transformation rate parameters, which can be incorporated into mathematical models for application to source area remedial design and performance assessment. The following conclusions can be drawn from this study:

- *Dhc* cell abundance and growth was linked to proximity to the PCE–DNAPL source zone.
- Source zone architecture influenced bioenhanced PCE–DNAPL dissolution, with greater localized PCE dissolution enhancements observed within the source zone ganglia regions compared to pool regions.
- *Geo*SZ exceeded *Dhc* cell numbers by an order-of-magnitude in the PCE–DNAPL source until electron acceptors (PCE and TCE) were depleted in late time, consistent with prevalent PCE-to-*cis*-DCE dechlorination throughout most of the experiment.
- Increased residence time due to flow interruptions stimulated *Dhc* growth and activity, and sustained dechlorination and ethene formation throughout the aquifer cell occurred, even after flow was reinitiated.
- The predominance of a *Dhc* strain carrying the *vcrA* gene corresponded to VC and ethene formation in the source zone.

- The most prevalent RDase gene in both the pooled and ganglia regions was *vcrA*, which consistently exceeded *Dhc* cell numbers.
- DNAPL saturation (i.e., pool and ganglia) influenced attachment of *Dhc*and *Geo*SZ cells, with dechlorinating cells predominately associated with the solid phase as long as electron donor was not limiting.

Acknowledgments

The authors would like to thank B. Amos, E. Suchomel, E. Chen, J. Costanza, J. Hatt, and K. Ritalahti for advice and assistance with this work. Funding for this study was provided by the Strategic Environmental Research and Development Program (SERDP) under Project ER-2129 (contract W912HQ-11-C-0068), Project ER-2311 (contract W912HQ-13-C-0011), and Project ER-2312 (contract W912HQ-13-C-0055). The content of this manuscript has not been subject to agency review and does not necessarily represent the view of the sponsoring agency.

References

Adamson, D.T., McDade, J.M., Hughes, J.B., 2003. Inoculation of a DNAPL source zone to initiate reductive dechlorination of PCE. Environ. Sci. Technol., 37 (11), 2525-2533.

Alfreider, A., Krössbacher, M., Psenner, R., 1997. Groundwater samples do not reflect bacterial densities and activity in subsurface systems. Water Res., 31 (4), 832-840.

Amos, B.K., Daprato, R.C., Hughes, J.B., Pennell, K.D., Löffler, F.E., 2007. Effects of the nonionic surfactant Tween 80 on microbial reductive dechlorination of chlorinated ethenes. Environ. Sci. Technol., 41, 1710-1716.

Amos, B.K., Suchomel, E.J., Pennell, K.D., Löffler, F.E., 2008. Microbial activity and distribution during enhanced contaminant dissolution from a NAPL source zone. Water Res., 42, 2963-2974.

Amos, B.K., Suchomel, E.J., Pennell, K.D., Löffler, F.E., 2009. Spatial and temporal distributions of *Geobacter lovleyi* and *Dehalococcoides* spp. during bioenhanced PCE–NAPL dissolution. Environ. Sci. Technol., 43 (6), 1977-1985.

Azizian, M.F., Behrens, S., Sabalowsky, A., Dolan, M.E., Spormann, A.M., Semprini L., 2008. Continuous-flow column study of reductive dehalogenation of PCE upon bioaugmentation with the Evanite enrichment culture. J. Contam. Hydrol., 100 (1–2), 11-21.

Balkwill, D.L., Ghiorse, W.C., 1985. Characterization of subsurface bacteria associated with two shallow aquifers in Oklahoma. Appl. Environ. Microbiol. 50 (3), 580–588.

Bekins, B., Godsy, E.,Warren, E., 1999. Distribution of microbial physiologic types in an aquifer contaminated by crude oil. Microb. Ecol. 37 (4), 263–275.

Butler, E.C., Hayes, K.F., 2001. Factors influencing rates and products in the transformation of trichloroethylene by iron sulfide and ironmetal. Environ. Sci. Technol. 35 (19), 3884–3891.

Cápiro, N.L., Da Silva, M.L.B., Stafford, B.P., Rixey, W.G., Alvarez, P.J.J., 2008. Microbial community response to a release of neat ethanol onto residual hydrocarbons in a pilot-scale aquifer tank. Environ. Microbiol. 10 (9), 2236–2244.

Cápiro, N.L., Wang, Y., Hatt, J.K., Lebrón, C.A., Pennell, K.D., Löffler, F.E., 2014. Distribution of organohalide-respiring bacteria between solid and aqueous phases. Environ. Sci. Technol. 48 (18), 10878–10887.

Christ, J.A., Abriola, L.M., 2007. Modeling metabolic reductive dechlorination in dense non-aqueous phase liquid source-zones. Adv. Water Resour. 30 (6–7), 1547–1561.

Christ, J.A., Ramsburg, C.A., Loeffler, F.E., Pennell, K.D., Abriola, L.M., 2005. Coupling aggressive mass removal with microbial reductive dichlorination for remediation of DNAPL source zones — a review and assessment. Environ. Health Perspect. 113 (4), 465–477 (doi: 410.1289/ehp.6932).

Christ, J.A., Ramsburg, C.A., Pennell, K.D., Abriola, L.M., 2010. Predicting DNAPL mass discharge from pool-dominated source zones. J. Contam. Hydrol. 114 (1–4), 18–34.

Chu, M., Kitanidis, P.K., McCarty, P.L., 2003. Effects of biomass accumulation on microbially enhanced dissolution of a PCE pool: a numerical simulation. J. Contam. Hydrol. 65 (1–2), 79–100.

Chu, M., Kitanidis, P.K., McCarty, P.L., 2004. Possible factors controlling the effectiveness of bioenhanced dissolution of non-aqueous phase tetrachloroethene. Adv.Water Resour. 27 (6), 601–615.

Cope, N., Hughes, J.B., 2001. Biologically-enhanced removal of PCE from NAPL source zones. Environ. Sci. Technol. 35 (10), 2014–2021.

Costanza, J., Flethcher, K.E., Löffler, F.E., Pennell, K.D., 2009. Fate of TCE in heated Fort Lewis soil. Environ. Sci. Technol. 43 (3), 909–914.

Da Silva, M.L., Daprato, R.C., Gomez, D.E., Hughes, J.B., Ward, C.H., Alvarez, P.J., 2006. Comparison of bioaugmentation and biostimulation for the enhancement of dense

nonaqueous phase liquid source zone bioremediation. Water Environ. Res. 78 (13), 2456–2465.

Damgaard, I., Bjerg, P.L., Bælum, J., Scheutz, C., Hunkeler, D., Jacobsen, C.S., Tuxen, N., Broholm, M.M., 2013a. Identification of chlorinated solvents degradation zones in clay till by high resolution chemical, microbial and compound specific isotope analysis. J. Contam. Hydrol. 146, 37–50.

Damgaard, I., Bjerg, P.L., Jacobsen, C.S., Tsitonaki, A., Kerrn-Jespersen, H., Broholm, M.M., 2013b. Performance of full-scale enhanced reductive dechlorination in clay till. Groundw. Monit. Remediat. 33 (1), 48–61.

Fennell, D.E., Carroll, A.B., Gossett, J.M., Zinder, S.H., 2001. Assessment of indigenous reductive dechlorinating potential at a TCE-contaminated site using microcosms, polymerase chain reaction analysis, and site data. Environ. Sci. Technol. 35 (9), 1830–1839.

Fletcher, K.E., Costanza, J., Pennell, K.D., Löffler, F.E., 2011. Electron donor availability for microbial reductive processes following thermal treatment. Water Res. 45 (20), 6625–6636.

Fontes, D.E., Mills, A.L., Hornberger, G.M., Herman, J.S., 1991. Physical and chemical factors influencing transport of microorganisms through porous media. Appl. Environ. Microbiol. 57 (9), 2473–2481.

Glover, K.C., Munakata-Marr, J., Illangasekare, T.H., 2007. Biologically enhanced mass transfer of tetrachloroethene from DNAPL source zones: experimental evaluation and influence of pool morphology. Environ. Sci. Technol. 41 (4), 1384–1389.

Godsy, E.M., Goerlitz, D.F., Grbic-Galic, D., 1992. Methanogenic biodegradation of creosote contaminants in natural and simulated ground-water ecosystems. Ground Water 30 (2), 232–242.

Haest, P.J., Philips, J., Springael, D., Smolders, E., 2011. The reactive transport of trichloroethene is influenced by residence time and microbial numbers. J. Contam. Hydrol. 119 (1–4), 89–98.

Haest, P.J., Springael, D., Seuntjens, P., Smolders, E., 2012. Self-inhibition can limit biologically enhanced TCE dissolution from a TCE DNAPL. Chemosphere 89 (11), 1369–1375.

Harkness, M., Fisher, A., 2013. Use of emulsified vegetable oil to support bioremediation of TCE DNAPL in soil columns. J. Contam.Hydrol. 151, 16–33.

Hazen, T., Jiménez, L., López de Victoria, G., Fliermans, C., 1991. Comparison of bacteria from deep subsurface sediment and adjacent groundwater. Microb. Ecol. 22 (1), 293–304.

He, J., Ritalahti, K.M., Yang, K.-L., Koenigsberg, S.S., Loffler, F.E., 2003. Detoxification of vinyl chloride to ethene coupled to growth of an anaerobic bacterium. Nature 424 (6944), 62–65.

Holm, P.E., Nielsen, P.H., Albrechtsen, H.J., Christensen, T.H., 1992. Importance of unattached bacteria and bacteria attached to sediment in determining potentials for degradation of xenobiotic organic contaminants in an aerobic aquifer. Appl. Environ. Microbiol. 58 (9), 3020–3026.

Krajmalnik-Brown, R., Hölscher, T., Thomson, I.N., Saunders, F.M., Ritalahti, K.M., Löffler, F.E., 2004. Genetic identification of a putative vinyl chloride reductase in Dehalococcoides sp. strain BAV1. Appl. Environ. Microbiol. 70 (10), 6347–6351.

Kueper, B.H., Stroo, H.F., Vogel, C.M., Ward, C.H., 2014. Chlorinated Solvent Source Zone Remediation. Springer, New York, NY, pp. 1–27.

Lehman, R.M., 2007. Understanding of aquifer microbiology is tightly linked to sampling approaches. Geomicrobiol J. 24 (3–4), 331–341.

Lehman, R.M., Colwell, F.S., Bala, G.A., 2001. Attached and unattached microbial communities in a simulated basalt aquifer under fracture- and porous-flow conditions. Appl. Environ. Microbiol. 67 (6), 2799–2809.

Liu, Y., Tay, J.-H., 2002. The essential role of hydrodynamic shear force in the formation of biofilm and granular sludge. Water Res. 36 (7), 1653–1665.

Löffler, F.E., Edwards, E.A., 2006. Harnesssing microbial activities for environmental cleanup. Curr. Opin. Biotechnol. 17 (3), 274–284.

Löffler, F.E., Sanford, R.A., Tiedje, J.M., 1996. Initial characterization of a reductive dehalogenase from Desulfitobacterium chlororespirans Co23. Appl. Environ. Microbiol. 62, 3809–3813.

Löffler, F.E., Yan, J., Ritalahti, K.M., Adrian, L., Edwards, E.A., Konstantinidis, K.T., Müller, J.A., Fullerton, H., Zinder, S.H., Spormann, A.M., 2013a. Dehalococcoides mccartyi gen. nov., sp. nov., obligately organohalide-respiring anaerobic bacteria relevant to halogen cycling and bioremediation, belong to a novel bacterial class, Dehalococcoidia classis nov., order Dehalococcoidales ord. nov. and family Dehalococcoidaceae fam. nov., within the phylum Chloroflexi. Int. J. Syst. Evol. Microbiol. 63 (Pt 2), 625–635.

Löffler, F.E., Ritalahti, K.M., Zinder, S.H., 2013b. Bioaugmentation for Groundwater Remediation. Springer, New York, NY, pp. 39–88.

Lu, X., Wilson, J.T., Kampbell, D.H., 2006. Relationship between Dehalococcoides DNA in ground water and rates of reductive dechlorination at field scale. Water Res. 40 (16), 3131–3140.

Lyon, D.Y., Vogel, T.M., 2013. Bioaugmentation for Groundwater Remediation. Springer, New York, NY, pp. 1–37.

Magnuson, J.K., Romine,M.F., Burris, D.R., Kingsley,M.T., 2000. Trichloroethene reductive dehalogenase from Dehalococcoides ethenogenes: sequence of tceA and substrate range characterization. Appl. Environ. Microbiol. 66 (12), 5141–5147.

McGuire, T., Hughes, J.B., 2003. Effects of surfactants on the dechlorination of chlorinated ethenes. Environ. Toxicol. Chem. 22 (11), 2630–2638.

Mravik, S.C., Sillan, R.K., Wood, A.L., Sewell, G.W., 2003. Field evaluation of the solvent extraction residual biotreatment technology. Environ. Sci. Technol. 37 (21), 5040–5049.

Müller, J.A., Rosner, B.M., von Abendroth, G.,Meshulam-Simon, G.,McCarty, P.L., Spormann, A.M., 2004. Molecular identification of the catabolic vinyl chloride reductase

fromDehalococcoides sp. strain vs and its environmental distribution. Appl. Environ. Microbiol. 70 (8), 4880–4888.

NRC, 2013. Alternatives for Managing the Nation's Complex Contaminated Groundwater Sites. The National Academies Press, Washington, DC.

Pandey, J., Chauhan, A., Jain, R.K., 2009. Integrative approaches for assessing the ecological sustainability of in situ bioremediation. FEMS Microbiol. Rev. 33 (2), 324–375.

Park, E., Parker, J.C., 2008. Effects of mass reduction, flow reduction and enhanced biodecay of DNAPL source zones. Transp. Porous Media 73 (1), 95–108.

Parker, J.C., Park, E., 2004. Modeling field-scale dense nonaqueous phase liquid dissolution kinetics in heterogeneous aquifers. Water Resour. Res. 40, W051091.

Pedersen, K., Ekendahl, S., 1990. Distribution and activity of bacteria in deep granitic groundwaters of southeastern sweden. Microb. Ecol. 20 (1), 37–52.

Pennell, K., Cápiro, N., Walker, D., 2014. Chlorinated Solvent Source Zone Remediation. In: Kueper, B.H., Stroo, H.F., Vogel, C.M., Ward, C.H. (Eds.), Springer, New York, pp. 353–394.

Philips, J., Hamels, F., Smolders, E., Springael, D., 2012. Distribution of a dechlorinating community in relation to the distance from a trichloroethene dense nonaqueous phase liquid in a model aquifer. FEMS Microbiol. Ecol. 81 (3), 636–647.

Philips, J., Van Muylder, R., Springael, D., Smolders, E., 2013. Electron donor limitations reduce microbial enhanced trichloroethene DNAPL dissolution: a flux-based analysis using diffusion-cells. Chemosphere 91 (1), 7–13.

Ramsburg, C.A., Abriola, L.M., Pennell, K.D., Loffler, F.E., Gamache, M.,Amos, B.K., Petrovskis, E.A., 2004. Stimulated microbial reductive dichlorination following surfactant treatment at the Bachman road site. Environ. Sci. Technol. 38 (22), 5902–5914.

Ramsburg, C.A., Thornton, C.E., Christ, J.A., 2010. Degradation product partitioning in source zones containing chlorinated ethene dense nonaqueous-phase liquid. Environ. Sci. Technol. 44 (23), 9105–9111.

Ramsburg, C.A., Christ, J.A., Douglas, S.R., Boroumand, A., 2011. Analytical modeling of degradation product partitioning kinetics in source zones containing entrapped DNAPL.Water Resour. Res. 47 (3).

Reardon, C.L., Cummings, D.E., Petzke, L.M., Kinsall, B.L., Watson, D.B., Peyton, B.M., Geesey, G.G., 2004. Composition and diversity of microbial communities recovered from surrogate minerals incubated in an acidic uranium-contaminated aquifer. Appl. Environ. Microbiol. 70 (10), 6037–6046.

Ritalahti, K.M., Hatt, J.K., Lugmayr, V., Henn, K., Petrovskis, E.A., Ogles, D.M., Davis, G.A., Yeager, C.M., Lebrón, C.A., Löffler, F.E., 2010a. Comparing on-site to off-site biomass collection for Dehalococcoides biomarker gene quantification to predict in situ chlorinated ethene detoxification potential. Environ. Sci. Technol. 44 (13), 5127–5133.

Ritalahti, K.M., Hatt, J.K., Petrovskis, E., Löffler, F.E., 2010b. Handbook of Hydrocarbon and Lipid Microbiology. Springer, pp. 3407–3418.

Schaefer, C.E., Condee, C.W., Vainberg, S., Steffan, R.J., 2009. Bioaugmentation for chlorinated ethenes using Dehalococcoides sp.: comparison between batch and column experiments. Chemosphere 75 (2), 141–148.

Schaefer, C.E., Towne, R.M., Vainberg, S., McCray, J.E., Steffan, R.J., 2010. Bioaugmentation for treatment of dense non-aqueous phase liquid in fractured sandstone blocks. Environ. Sci. Technol. 44 (13), 4958–4964.

Scholl, M.A., Mills, A.L., Herman, J.S., Hornberger, G.M., 1990. The influence of mineralogy and solution chemistry on the attachment of bacteria to representative aquifer materials. J. Contam. Hydrol. 6 (4), 321–336.

Sleep, B.E., Seepersad, D.J., Mo, K., Heidorn, C.M., Hrapovic, L., Morrill, P.L., McMaster, M.L., Hood, E.D., Lebron, C., Sherwood Lollar, B., Major, D.W., Edwards, E.A., 2006. Biological enhancement of tetrachloroethene dissolution and associatedmicrobial community changes. Environ. Sci. Technol. 40 (11), 3623–3633.

Stroo, H.F., Leeson, A., Marqusee, J.A., Johnson, P.C.,Ward, C.H., Kavanaugh,M.C., Sale, T.C., Newell, C.J., Pennell, K.D., Lebron, C.A., Unger, M., 2012. Chlorinated ethene source remediation: lessons learned. Environ. Sci. Technol. 46 (12), 6438–6447.

Suchomel, E.J., Pennell, K.D., 2006. Reductions in contaminant mass discharge following partial mass removal from DNAPL source zones. Environ. Sci. Technol. 40, 6110–6116.

Suchomel, E.J., Ramsburg, C.A., Pennell, K.D., 2007. Evaluation of trichloroethene

recovery processes in heterogeneous aquifer cells flushed with biodegradable surfactants. J. Contam. Hydrol. 94, 195–214.

Sung, Y., Ritalahti, K.M., Sanford, R.A., Urbance, J.W., Flynn, S.J., Tiedje, J.M., Löffler, F.E., 2003. Characterization of two tetrachloroethene-reducing, acetateoxidizing anaerobic bacteria, and their description as Desulfuromonas michiganensis sp. nov. Appl. Environ. Microbiol. 69 (5), 2964–2974.

Sung, Y., Fletcher, K.E., Ritalahti, K.M., Apkarian, R.P., Ramos-Hernández, N., Sanford, R.A., Mesbah, N.M., Löffler, F.E., 2006a. Geobacter lovleyi sp. nov. strain SZ, a novel metal-reducing and tetrachloroethene-dechlorinating bacterium. Appl. Environ. Microbiol. 72 (4), 2775–2782.

Sung, Y., Ritalahti, K.M., Apkarian, R.P., Löffler, F.E., 2006b. Quantitative PCR confirms purity of strain GT, a novel trichloroethene-to-ethene-respiring Dehalococcoides isolate. Appl. Environ. Microbiol. 72 (3), 1980–1987.

Thomas, W.E., Trintchina, E., Forero, M., Vogel, V., Sokurenko, E.V., 2002. Bacterial adhesion to target cells enhanced by shear force. Cell 109 (7), 913–923.

Tidwell, V.C., Glass, R., 1994. X-ray and visible light transmission for laboratory measurement of two-dimensional saturation fields in thin-slab systems. Water Resour. Res. 30, 2873–2882.

van der Zaan, B., Hannes, F., Hoekstra, N., Rijnaarts, H., de Vos, W.M., Smidt, H., Gerritse, J., 2010. Correlation of Dehalococcoides 16S rRNA and chloroethene-reductive dehalogenase geneswith geochemical conditions in chloroethene-contaminated groundwater. Appl. Environ. Microbiol. 76 (3), 843–850.

Yang, Y., McCarty, P.L., 2000. Biologically enhanced dissolution of tetrachloroethene DNAPL. Environ. Sci. Technol. 34 (14), 2979–2984.

Yang, Y., McCarty, P.L., 2002. Comparison between donor substrates for biologically enhanced tetrachloroethene DNAPL dissolution. Environ. Sci. Technol. 36 (15), 3400–3404.

Zhang, H., Olson, M., 2012. Effect of heavy metals on bacterial attachment in soils. J. Environ. Eng. 138 (11), 1106–1113.

Zheng, D., Carr, C.S., Hughes, J.B., 2001. Influence of hydraulic retention time on extent of PCE dechlorination and preliminary characterization of the enrichment culture. Bioremediat. J. 5 (2), 159–168.

SUPPLEMENTARY MATERIAL

Spatial and Temporal Dynamics of Organohalide-Respiring Bacteria in a Heterogeneous PCE-DNAPL Source Zone

Natalie L. Cápiro [1,*], Frank E. Löffler [2,3,4,5], and Kurt D. Pennell [1,*]

[1]Department of Civil and Environmental Engineering, Tufts University, Medford, MA 02155

[2] Department of Microbiology, University of Tennessee, Knoxville, TN 37996

[3] Department of Civil and Environmental Engineering, University of Tennessee, Knoxville, TN 37996

[4] Center for Environmental Biotechnology, University of Tennessee, Knoxville, TN 37996

[5] University of Tennessee and Oak Ridge National Laboratory (UT-ORNL) Joint Institute for Biological Sciences (JIBS) and Biosciences Division, Oak Ridge National Laboratory, Oak Ridge, TN 37831.

***Corresponding authors:**

Telephone: 617-627-6015; Fax: 607-627-3994; Email: natalie.capiro@tufts.edu (N.L. Cápiro)
Telephone: 617-627-3099; Fax: 607-627-3994; Email: kurt.pennell@tufts.edu (K.D. Pennell)

Number of pages: 15

Number of tables: 2

Number of figures: 2

Chemicals and porous media

PCE (ACS Grade ≥99% purity), which has an equilibrium aqueous solubility of ca. 1,200 μM (200 mg/L) (Taylor et al. 2001) and a density of 1.62 g/cm^3 (Schwarzenbach et al. 2005), was obtained from Sigma Aldrich (St. Louis, MO). In order to visualize PCE-DNAPL, the lipophilic dye Oil-Red-O (Fisher Scientific) was added at a concentration of 4 x 10^{-4} M, which has been shown to have minimal effects on relevant physical-chemical properties of PCE (Taylor et al. 2001). Polyoxyethylene (20) sorbitan monooleate (Tween® 80), a nonionic, biodegradable surfactant capable of substantial DNAPL solubilization with minimal free product mobilization (Ramsburg et al. 2005, Suchomel et al. 2007) was obtained from Uniqema (New Castle, DE; Lot # 2398A). Tween® 80 has a density and molar mass of 1.07 g/mL and 1,310 g/mol, respectively, and a critical micelle concentration (CMC) of approximately 35 mg/L (Pennell and Abriola 1997). Influent solutions of Tween® 80 were prepared at a concentration of 4% (w/w), or approximately 40,000 mg/L. The aqueous surfactant solutions were amended with NaBr (1,000 mg/L; Fisher Scientific) as a non-reactive tracer and dyed with Erioglaucine A (Fluka Chemical) dye at a concentration of 3×10^{-5} M to visualize delivery of surfactant solution to the aquifer cell. Surfactant-free solutions used prior to bioaugmentation were prepared with $CaCl_2$•$2H_2O$ (500 mg/L; Fisher Scientific) as the background electrolyte. All aqueous solutions were prepared with degassed, de-ionized (DI) water (Nanopure Barnstead/Thermolyne Corp., Dubuque, IA).

A 1:1 mixture of two size fractions of Accusand (20-30 and 40-50 mesh) (Unimin Corp., New Canaan, CT) was selected as the background porous medium for the aquifer cells based on their well characterized properties (Scroth et al. 1996) and demonstrated effectiveness in prior light transmission studies (Suchomel and Pennell 2006). F-70 Ottawa sand (40-270 mesh) was

obtained from U.S. Silica Co. (Berkeley Springs, WV) and was used to create lower permeability lenses within the higher permeability background medium. The intrinsic permeability of F-70 Ottawa sand is approximately 8.2 x 10^{-12} m^2, while the 1:1 mixture of 20-30 mesh Accusand and 40-50 mesh Accusand has an intrinsic permeability of approximately 1.6 x 10^{-11} m^2 (Scroth et al. 1996).

Biological sample preparation and DNA extraction

Biomass was collected from 15 mL aqueous effluent samples by centrifugation at 4°C for 30 minutes at 4,000 rpm in a table top refrigerated centrifuge (Eppendorf 5810R, Hauppauge, NY). All but ca. 1 mL of the supernatant was decanted, and the cell pellet was suspended in the remaining liquid. Centrifugation was repeated at 13,200 rpm for 15 minutes. From the side ports, 1-1.25 mL liquid samples were collected using a 2.5 mL glass syringe (Hamilton Co., Reno, NV) and centrifuged at 13,200 rpm at room temperature for 15 minutes. After removing the supernatant, the pellets were stored at -20°C until genomic DNA was extracted using the DNeasy® Blood and Tissue Kit (Qiagen, Valencia, CA) according the bacterial protocol, with modifications previously described by Ritalahti et al. (2006). DNA was obtained in final volumes of 400 µL buffer AE (provided with the DNeasy® Blood and Tissue Kit) and stored at -80°C until qPCR analysis. Soil was collected through destructive sampling in a 1cm radius around each of the 18 side port locations at the termination of the experiment and prepared for DNA extraction according to described protocols (Cápiro et al. 2008). After homogenizing the samples, 1-3 g of the wet sample was placed in an aluminum weighing tray and dried overnight at 100°C to determine the samples' water content. DNA was extracted from 0.27-0.33 g of wet sample (0.22-0.27 g dry weight) solid material using the PowerSoil™ DNA Isolation Kit

(MoBio Laboratories, Inc., Carlsbad, CA) in accordance with the procedures provided by the manufacturer. DNA was obtained in a final volume of 100 µL in solution C6 (provided with the PowerSoil™ Isolation Kit) and stored at -80°C until qPCR analysis.

Quantitative real-time PCR (qPCR) analysis

Dhc strains and *Geo*SZ cell numbers were quantified using triplicate qPCR reactions targeting the 16S rRNA genes with an ABI 7500 Fast Real-Time PCR System (Applied Biosystems, Foster City, CA) under the standard operating modes. Primers and probes used were obtained from IDT Technologies (Coralville, IA). TaqMan-based qPCR analysis was used to quantify total *Dhc* 16S rRNA gene copies and associated reductive dehalogenase (RDase) genes (Ritalahti et al. 2006), and quantification of *Geo*SZ 16S rRNA gene copies was performed using SYBR Green detection chemistry according to described protocols (Amos et al. 2007b, Duhamel and Edwards 2006) with the modifications introduced by Amos et al. (2009).

Dhc cell numbers were expressed in terms of 16S rRNA gene copies or cell numbers per mL of fluid or per gram of sand/soil and used interchangeably because the known *Dhc* strains contain a single 16S rRNA gene copy per genome (Kube et al. 2005, Seshadri et al. 2005). The genome of *Geo*SZ contains two 16S rRNA gene copies (www.jgi.doe.gov) (Wagner et al. 2012); therefore, gene copy numbers were divided by a factor of two to yield the cell numbers that were reported per mL of fluid or per gram of solid. Standard curves were generated following the procedure outlined by Ritalahti et al. (2006) using 10-fold dilutions of quantified plasmids (concentration determined spectrophotometrically at 260 nm) carrying a single copy of the 16S rRNA gene of either *Dhc* strain BAV1 or *Geo*SZ.

Analytical methods

Aqueous-phase samples (1 mL) were analyzed for chlorinated ethenes as described (Amos et al. 2007a) with a Hewlett-Packard (HP) 7694 headspace autosampler connected to a HP 6890 gas chromatograph (GC) equipped with a HP-624 column (60 m by 0.32 mm i.d.; film thickness, 1.8 μm) and a flame ionization detector (FID). Chlorinated ethenes and ethene standard curves were prepared as described (Gossett 1987, Löffler et al. 1997). The pH of column effluent was measured using a VWR Model 8000 pH meter (#511710, VWR Scientific, West Chester, Pennsylvania) equipped with an Accumet gel-filled pH combination electrode (#13-620-290, Fisher Scientific). Organic acids were measured using a Waters High Performance Liquid Chromatography (HPLC) system (Waters, Corp., Milford, Massachusetts) equipped with a Waters 2487 dual-wavelength absorbance detector set at 210 nm and a Waters 717 plus autosampler as described (He et al. 2003). Analysis of Tween 80 was performed using an Agilent 1100 series HPLC equipped with diode array detector (DAD) and a Sedex 55 Evaporative Light Scattering Detector (ELSD) based on methods described by Taylor et al. (2001).

The source zone DNAPL saturation distribution of the aquifer cell was quantified using a light transmission (LT) system (Suchomel and Pennell 2006) that was based on the design of Tidwell and Glass (1994). A Nikon Coolpics 900 digital camera was used to capture digital images of the aquifer cells that were illuminated from behind with a Flathead 80 light bank (Kino Flo Inc., Burbank, CA) containing eight 48in 75W KF32 fluorescent bulbs (Kino Flo Inc.). All exterior lights were extinguished during imaging to ensure that lighting conditions were consistent during image acquisition. Digital images were processed using Adobe Photoshop ver. 7.0.1.

Thickness-averaged saturation distributions were calculated on a pixel basis (ca. 0.3 mm × 0.3 mm) using MATLAB 7.8 software (MathWorks, Inc. Natick MA), and integrated over the entire source zone region to estimate the total DNAPL source zone volume. Local DNAPL saturations were estimated by comparison of the digital image to generated hue-NAPL saturation calibration curves, which were developed using an experimental method adapted from Darnault et al. (1998). Residual saturation cutoff between PCE-DNAPL pools and ganglia in the background porous medium was determined experimentally using one-dimensional columns and procedures described by Pennell et al. (1996).

Abiotic plume development and surfactant flushing

After the introduction of the PCE-DNAPL in the aquifer cell, aqueous PCE concentrations were monitored throughout the plume development period, including during the two surfactant flushes with 4% (wt.) Tween 80 solution, and following bioaugmentation (Figure 2). Figure S-1 shows the PCE measured during the abiotic portion of experiment (till ca. PV 78). Prior to the first surfactant flush, the downgradient plume and flux-averaged effluent concentrations approached the aqueous solubility of PCE (>0.9 mM). PCE concentrations spiked at 5.5mM and 1.6mM following surfactant flush #1 (PV 5.2) and surfactant flush #2 (PV 32.3), respectively (Figure S-1). This enhanced surfactant PCE solubilization behavior is consistent with the findings of numerous previous studies (Dwarakanath et al. 1999, Jafvert et al. 1994, Suchomel and Pennell 2006, Suchomel et al. 2007, Taylor et al. 2001). After the second surfactant flush, flux-averaged effluent PCE concentration dropped to 0.3mM. The resulting PCE source zone architecture and saturation distribution prior to bioaugmentation are shown in Figure S-2.

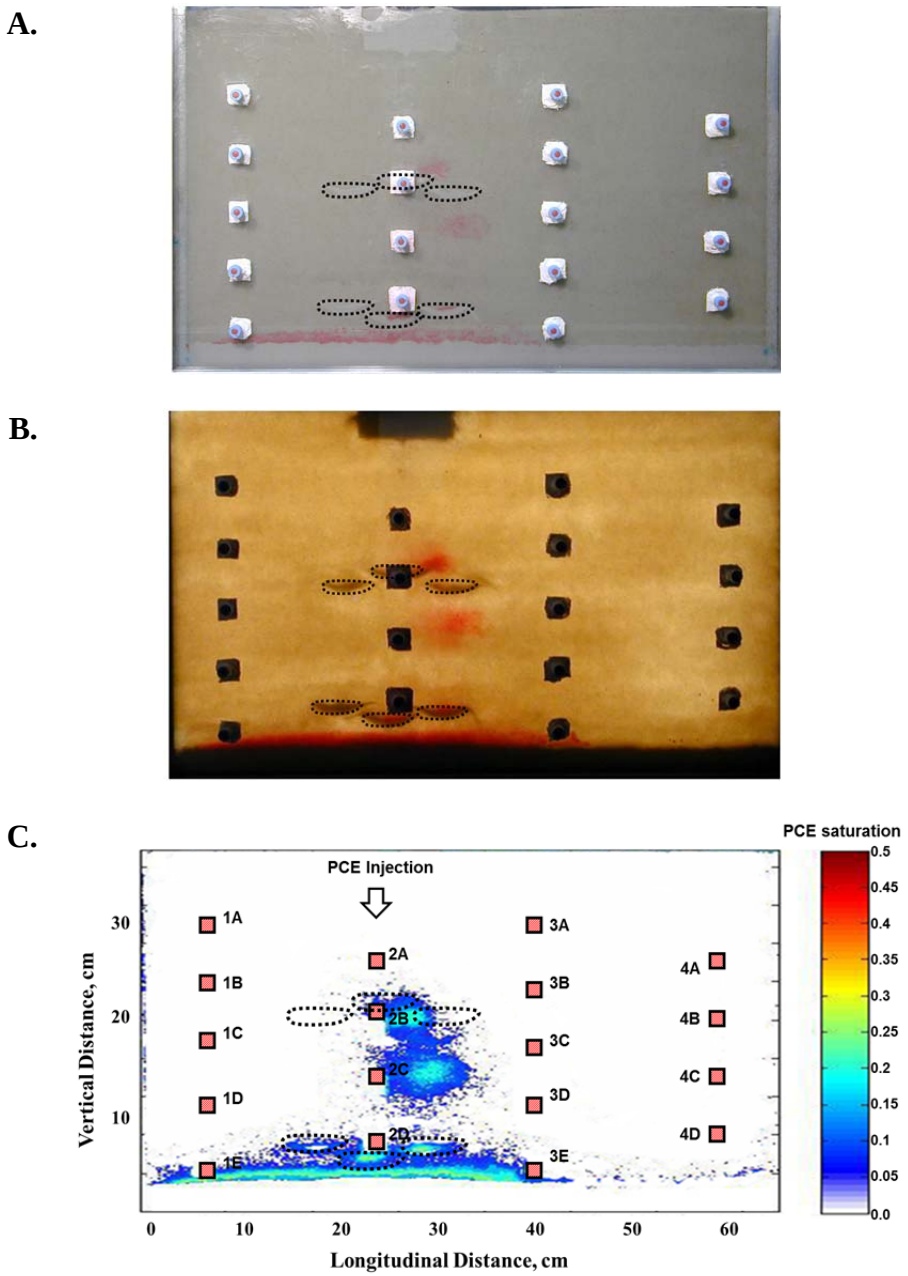

Figure S-1: **A.** Photograph of the aquifer cell under laboratory lighting conditions. **B.** Light transmission image of the aquifer cell showing DNAPL distribution. **C.** MATLAB (v. 7.8) processed light transmission of the source zone showing DNAPL saturation following surfactant flushing, flushing with 25 PVs of $CaCl_2$ electrolyte solution, and prior to bioaugmentation (PV 58), GTP= 1.04 and PF= 0.49. Locations of low the permeability lenses (F-70 Ottawa sand) are outlined with dotted lines near ports 2B and 2D.

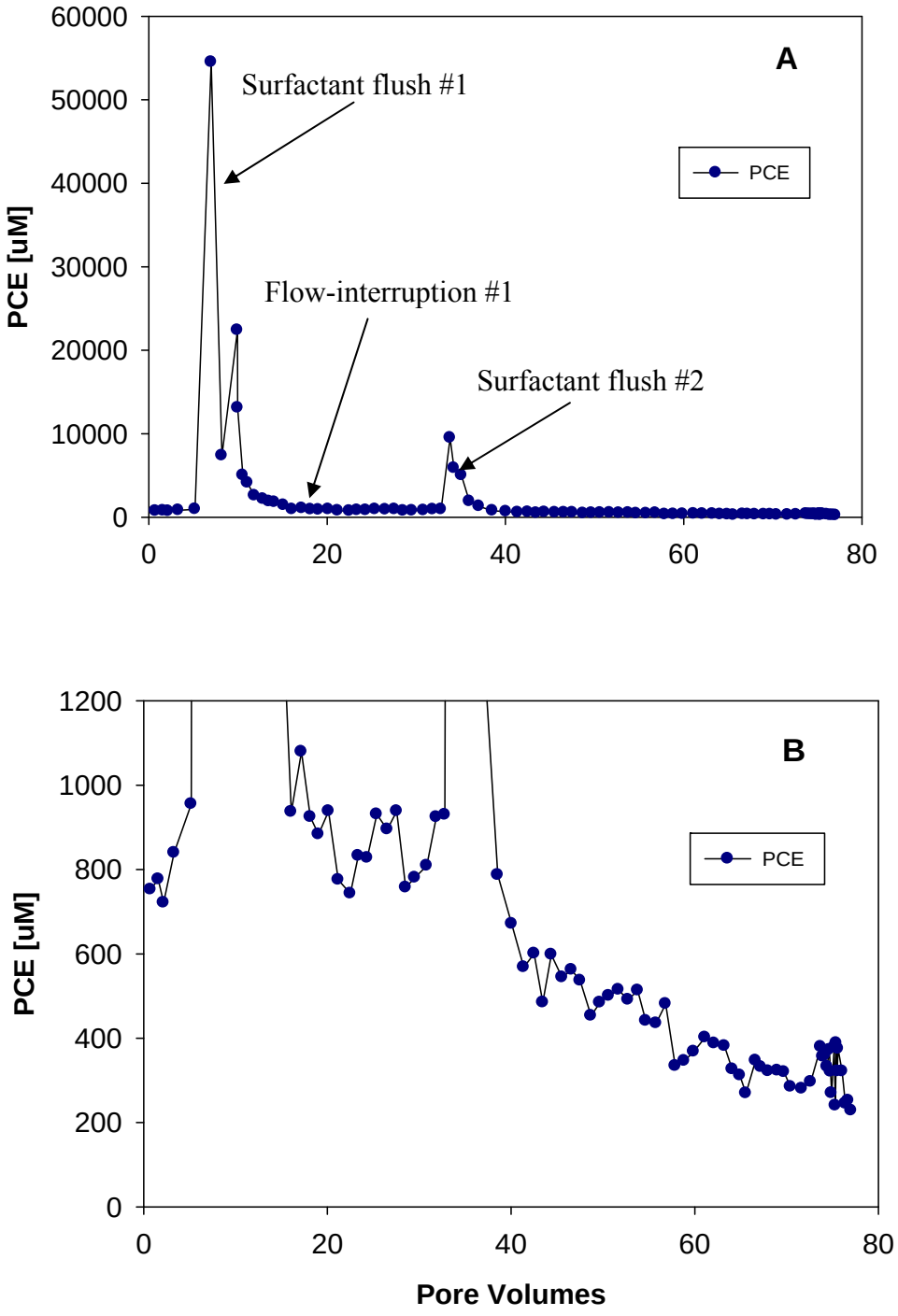

Figure S-2: Effluent PCE concentrations prior to aquifer cell bioaugmentation. **A.)** Depicts the PCE concentrations during surfactant flushing, and **B.)** shows the PCE concentrations during prior to bioaugmentation with the y-axis from graph A truncated to the aqueous solubility of PCE.

Measurement of dechlorinating bacteria in pool and ganglia zones

Within the representative pool (port 3E) and ganglia (port 4D) regions of the aquifer cell non-attached (planktonic) *Dhc* and *GeoSZ* cells were measured periodically following bioaugmentation (PV 77.5) till the termination of the experiment (PV 116). The relative distribution of these two dechlorinating microbial species is presented in Table S-1. Here, the benefit of increased hydraulic retention time resulting from the two flow interruptions (PVs 106.6 and 113) is highlighted with an increased fraction of *Dhc* cells that persisted till the termination of the experiment (PV 116). Within the pool and ganglia regions, RDase genes coincided with the formation of vinyl chloride and ethene, and revealed that the *vcrA* gene consisting exceeded the total *Dhc* 16S rRNA genes (Figure 5 and Table S-2).

Table S-1: Dechlorinating bacteria in the pool region (Port 3E) and ganglia region (Port 4D).

	Pool Region (Port 3E)			***Ganglia Region (Port 4D)***		
PV	Total dechlorinators (cells/mL)	Fraction *Dhc*	Fraction *Geo*SZ	Total dechlorinators (cells/mL)	Fraction *Dhc*	Fraction *Geo*SZ
78.7	5.3E+05	0.01	0.99	1.4E+05	0.27	0.73
82.0	2.8E+07	0.00	1.00	8.6E+06	0.00	1.00
85.6	9.0E+05	0.00	1.00	1.3E+06	0.00	1.00
90.2	1.1E+08	0.00	1.00	1.1E+07	0.03	0.97
98.4	3.4E+08	0.02	0.98	4.4E+05	0.06	0.94
105.2	6.9E+06	0.01	0.99	1.5E+06	0.01	0.99
106.4	1.2E+08	0.02	0.98	1.2E+08	0.09	0.91
106.6	1.6E+08	0.15	0.85	4.5E+07	0.06	0.94
111.0	6.3E+07	0.07	0.93	3.4E+06	0.13	0.87
113.0	1.4E+07	0.12	0.88	2.9E+06	0.24	0.76
116.0	1.2E+08	0.84	0.16	3.2E+06	0.86	0.14

Table S-2: Fraction of *Dhc* cells and each RDase gene with respect to total RDase genes measured in the pool (Port 3E) and ganglia (Port 4D) regions.

Pooled Region (Port 3E)				
PV	**% *Dhc***	**% *tceA***	**% *vcrA***	**% *bvcA***
78.7	22%	2%	96%	2%
82	5%	5%	94%	1%
85.6	61%	22%	63%	15%
90.2	6%	30%	70%	0%
98.4	21%	54%	46%	0%
105.2	20%	6%	94%	0%
106.4	51%	21%	79%	0%
106.6	150%	13%	87%	0%
111	25%	33%	67%	0%
113	22%	38%	62%	0%
116.2	74%	36%	64%	0%
Avg	42%	23%	76%	2%
st dev	41%	16%	16%	4%

Ganglia Region (Port 4D)				
PV	**% *Dhc***	**% *tceA***	**% *vcrA***	**% *bvcA***
78.7	19%	1%	99%	0%
82	2%	14%	85%	1%
85.6	39%	32%	47%	21%
90.2	4%	5%	95%	0%
98.4	14%	1%	99%	0%
105.2	16%	9%	90%	0%
106.4	48%	4%	96%	0%
106.6	20%	1%	99%	0%
111	35%	4%	96%	0%
113	19%	34%	66%	0%
116.2	29%	34%	66%	0%
Avg	22%	10%	87%	2%
st dev	14%	12%	16%	6%

Supplementary material references

Amos, B.K., Christ, J.A., Abriola, L.M., Pennell, K.D. and Löffler, F.E. (2007a) Experimental evaluation and mathematical modeling of microbially enhanced tetrachloroethene (PCE) dissolution. Environmental Science & Technology 41, 963-970.

Amos, B.K., Suchomel, E.J., Pennell, K.D. and Löffler, F.E. (2009) Spatial and temporal distributions of *Geobacter lovleyi* and *Dehalococcoides* spp. during bioenhanced PCE-NAPL dissolution. Environmental Science & Technology 43(6), 1977-1985.

Amos, B.K., Sung, Y., Fletcher, K.E., Gentry, T.J., Wu, W.M., Criddle, C.S., Zhou, J. and Löffler, F.E. (2007b) Detection and quantification of *Geobacter lovleyi* strain SZ: Implications for bioremediation at tetrachloroethene- and uranium-impacted sites. Applied and Environmental Microbiology 73(21), 6898-6904.

Cápiro, N.L., M.L.B., D.S., Stafford, B.P., Rixey, W.G. and Alvarez, P.J.J. (2008) Microbial community response to a release of neat ethanol onto residual hydrocarbons in a pilot-scale aquifer tank. Environmental Microbiology 10(9), 2236–2244.

Darnault, C.J.G., Throop, J.A., DiCarlo, D.A., Rimmer, A., Steenhuis, T.S. and Parlange, J.Y. (1998) Visualization by light transmission of oil and water contents in transient two-phase flow fields. Journal of Contaminant Hydrology 31(3-4), 337-348.

Duhamel, M. and Edwards, E.A. (2006) Microbial composition of chlorinated ethene-degrading cultures dominated by *Dehalococcoides*. FEMS Microbiology Ecology 58, 538-549.

Dwarakanath, V., Kostarelos, K., Pope, G.A., Shots, D. and Wade, W.H. (1999) Anionic surfactant remediation of soil columns contaminated by nonaqueous phase liquids. Journal of Contaminant Hydrology 38(4), 465-488.

Gossett, J.M. (1987) Measurement of Henry's law constants for C_1 and C_2 chlorinated hydrocarbons. Environmental Science & Technology 21, 202-208.

He, J., Ritalahti, K.M., Aiello, M.R. and Löffler, F.E. (2003) Complete detoxification of vinyl chloride (VC) by an anaerobic enrichment culture and identification of the reductively dechlorinating population as a *Dehalococcoides* species. Applied and Environmental Microbiology 69(2), 996-1003.

Jafvert, C.T., van Hoof, P.L. and Heath, J.K. (1994) Solubilization of non-polar compounds by non-ionic surfactant micelles. Water Research 28(5), 1009-1017.

Kube, M., Beck, A., Zinder, S.H., Kuhl, H., Reinhardt, R. and Adrian, L. (2005) Genome sequence of the chlorinated compound respiring bacterium *Dehalococcoides* species strain CBDB1. Nature Biotechnology 23(10), 1269-1273.

Löffler, F.E., Champine, J.E., Ritalahti, K.M., Sprague, S.J. and Tiedje, J.M. (1997) Complete reductive dechlorination of 1,2-dichloropropane by anaerobic bacteria. Applied and Environmental Microbiology 63, 2870-2875.

Pennell, K.D. and Abriola, L.M. (1997) Bioremediation: Principles and Practice. Sikdar, S.K. and R.L.Irvine (eds), pp. 693-750, Technomic Publ., Lancaster, PA.

Pennell, K.D., Abriola, L.M. and Pope, G.A. (1996) Influence of viscous and buoyancy forces on the mobilization of residual tetrachloroethylene during surfactant flushing. . Environmental Science & Technology 30, 1328-1335.

Ramsburg, C.A., Pennel, K.D., Abriola, L.M., Daniels, G., Drummond, C.D., Gamache, M., Hsu, H.-L., Petrovskis, E.A., Rathfelder, K.M., Ryder, J.L. and Yavaraski, T.P. (2005) Pilot-scale demonstration of surfactant-enhanced PCE solubilization at the Bachman

Road site. 2. System operation and evaluation. Environmental Science & Technology, DOI: 10.1021/es049563r.

Ritalahti, K.M., Amos, B.K., Sung, Y., Wu, Q., Koenigsberg, S.S. and Löffler, F.E. (2006) Quantitative PCR targeting 16S rRNA and reductive dehalogenase genes simultaneously monitors multiple *Dehalococcoides* strains. Applied and Environmental Microbiology 72(4), 2765-2774.

Schwarzenbach, R.P., Gschwend, P.M. and Imboden, D.M. (2005) Environmental Organic Chemistry, John Wiley & Sons, Inc., Hoboken, NJ, USA.

Scroth, M.H., Ahearn, S.J., Selker, J.S. and Istok, J.D. (1996) Characterization of Miller-Similar Silica Sands for Laboratory Hydrologic Studies. Soil Science Society of America Journal 60, 1331-1339.

Seshadri, R., Adrian, L., Fouts, D.E., Eisen, J.A., Phillippy, A.M., Methe, B.A., Ward, N.L., Nelson, W.C., Deboy, R.T., Khouri, H.M., Kolonay, J.F., Dodson, R.J., Daugherty, S.C., Brinkac, L.M., Sullivan, S.A., Madupu, R., Nelson, K.T., Kang, K.H., Impraim, M., Tran, K., Robinson, J.M., Forberger, H.A., Fraser, C.M., Zinder, S.H. and Heidelberg, J.F. (2005) Genome sequence of the PCE-dechlorinating bacterium *Dehalococcoides ethenogenes*. Science 307(5706), 105-108.

Suchomel, E.J. and Pennell, K.D. (2006) Reductions in contaminant mass discharge following partial mass removal from DNAPL source zones. Environmental Science & Technology 40, 6110-6116.

Suchomel, E.J., Ramsburg, C.A. and Pennell, K.D. (2007) Evaluation of trichloroethene recovery processes in heterogeneous aquifer cells flushed with biodegradable surfactants. Journal of Contaminant Hydrology 94, 195-214.

Taylor, T.P., Pennell, K.D., Abriola, L.M. and Dane, J.H. (2001) Surfactant enhanced recovery of tetrachloroethylene from a porous medium containing low permeability lenses. 1. Experimental Studies. Journal of Contaminant Hydrology 48(3-4), 325-350.

Tidwell, V.C. and Glass, R. (1994) X-ray and visible light transmission for laboratory measurement of two-dimensional saturation fields in thin-slab systems. . Water Resources Research 30, 2873-2882.

Wagner, D.D., Hug, L.A., Hatt, J.K., Spitzmiller, M.R., Padilla-Crespo, E., Ritalahti, K.M., Edwards, E.A., Konstantinidis, K.T. and Löffler, F.E. (2012) Genomic determinants of organohalide-respiration in Geobacter lovleyi, an unusual member of the Geobacteraceae. BMC genomics 13(1), 200.